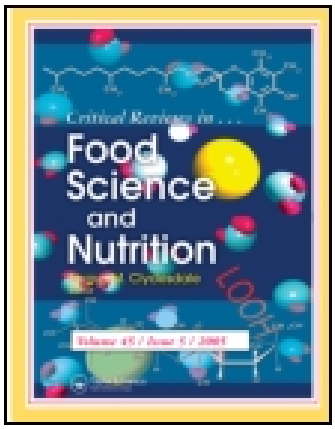

Critical Reviews in Food Science and Nutrition
Publication details, including instructions for authors and subscription information:
http://www.tandfonline.com/loi/bfsn20

Application of Hyperspectral Imaging in Food Safety Inspection and Control: A Review

Yao-Ze Feng [a] & Da-Wen Sun [a]
[a] Food Refrigeration and Computerized Food Technology (FRCFT), School of Biosystems Engineering , University College Dublin, National University of Ireland, Agriculture and Food Science Centre , Belfield , Dublin , Ireland
Published online: 24 Jul 2012.

To cite this article: Yao-Ze Feng & Da-Wen Sun (2012) Application of Hyperspectral Imaging in Food Safety Inspection and Control: A Review, Critical Reviews in Food Science and Nutrition, 52:11, 1039-1058, DOI: 10.1080/10408398.2011.651542

To link to this article: http://dx.doi.org/10.1080/10408398.2011.651542

Critical Reviews in Food Science and Nutrition, 52:1039–1058 (2012)

ISSN: 1040-8398 / 1549-7852 online
DOI: 10.1080/10408398.2011.651542

Taylor & Francis
Taylor & Francis Group

Application of Hyperspectral Imaging in Food Safety Inspection and Control: A Review

YAO-ZE FENG and DA-WEN SUN

Food Refrigeration and Computerized Food Technology (FRCFT), School of Biosystems Engineering, University College Dublin, National University of Ireland, Agriculture and Food Science Centre, Belfield, Dublin, Ireland

Food safety is a great public concern, and outbreaks of food-borne illnesses can lead to disturbance to the society. Consequently, fast and nondestructive methods are required for sensing the safety situation of produce. As an emerging technology, hyperspectral imaging has been successfully employed in food safety inspection and control. After presenting the fundamentals of hyperspectral imaging, this paper provides a comprehensive review on its application in determination of physical, chemical, and biological contamination on food products. Additionally, other studies, including detecting meat and meat bone in feedstuffs as well as organic residue on food processing equipment, are also reported due to their close relationship with food safety control. With these applications, it can be demonstrated that miscellaneous hyperspectral imaging techniques including near-infrared hyperspectral imaging, fluorescence hyperspectral imaging, and Raman hyperspectral imaging or their combinations are powerful tools for food safety surveillance. Moreover, it is envisaged that hyperspectral imaging can be considered as an alternative technique for conventional methods in realizing inspection automation, leading to the elimination of the occurrence of food safety problems at the utmost.

Keywords nondestructive method, hyperspectral imaging, chemical imaging, chemometrics, NIRS, computer vision, fluorescence, Raman, food safety, pathogen, contamination, fruits, vegetables, meat

INTRODUCTION

As a global issue, food safety is receiving increasing attention in both developed and developing countries. However, in spite of its high prevalence and importance, there is no direct scientific definition for food safety available. Food safety is normally described as the converse of food risk, that is, a discipline aiming to ensure that food is safe enough "from-farm-to-fork" for consumers so that outbreaks of food-borne illness can be reduced (Wilcock et al., 2004). The content of food safety involves a wide range: physical, chemical, and biological contamination and other associated hazards or poisons. In physical contamination, of particular concerns are fecal contaminations and defects that are closely linked to harmful pathogens, as well as abnormalities. Others may include the presence of foreign materials (such as stones from the environment, metals and glasses from the apparatus, finger nails from the processors, bone fragments in deboned meat, etc.). In terms of chemical contamination, several groups can be compartmentalized into natural toxins, food additives, agrochemical residues, hazards from food processing, and so on. Chemical contaminations are of great concern because the impact from them is incognizable in the early stage and is accumulative in nature, causing very severe (even fatal) consequences. More importantly, these harmful chemicals cannot be eliminated effectively by treatments that are useful in suppressing risks from microbiological contamination. On the other hand, microbiological contamination is the most common source of food-borne outbreaks, which consists of bacterial, fungal, virus, protozoa, and parasite contamination, where various pathogens and their metabolic toxins serve as the main culprits.

Food safety problems are frequently confronted in our daily life. Centers for Disease Control and Prevention (CDC) estimated that about 48 million food safety incidents take place annually in the USA, where around 128,000 are hospitalized and 3000 are dead (CDC, 2011). Any occurrence of food safety problems always brings substantial influence to the society, and governing bodies worldwide are taking strict measures to implement effective practices and policies for the surveillance of the food industry. Therefore analytical techniques play a

Address correspondence to Da-Wen Sun, Food Refrigeration and Computerized Food Technology (FRCFT), School of Biosystems Engineering, University College Dublin, National University of Ireland, Agriculture and Food Science Centre, Belfield, Dublin, Ireland. E-mail: dawen.sun@ucd.ie

critical role. However, current methods readily available as standard references are mostly destructive and slow. In order to overcome this, nondestructive methods, especially those based on optical properties, are urgently required.

Vibration spectroscopy (Sun, 2009) is an optical technology that depends on the interaction between incident light and molecules in matters. Because different molecules are sensitive to light with different wavelengths in terms of light absorption or scattering, the resultant spectra then record the information of these molecules over corresponding wavelengths (Cen and He, 2007; Lu et al., 2011; Sowoidnich et al., 2010). In other words, by scrutinizing the changes of spectra, one can reach the physical, chemical, and biological information within the products. However, spectrometers only detect a small portion of the samples; therefore, the spectra, strictly speaking, are sometimes not representative for the whole sample, especially when the ingredients are not evenly distributed. In order to obtain spatial information, another technology, that is, computer vision is available. Computer vision (Sun, 2008) imitates the principle of human vision, using three bands (red, green, and blue) to acquire the characteristics of objects. Working in visible range, the features obtained by computer vision include shape, color, size, and texture (Sun, 2000; Du and Sun, 2004; Zheng et al., 2006a; 2006b; Wu et al., 2008). However, only occasionally is this method reported to be sufficient for detecting chemical and biological parameters (Chmiel et al., 2011; Mohebbi et al., 2009). Both spectroscopy and computer vision techniques have found a wide range of applications in the food industry (Brosnan and Sun, 2004; Cubero et al., 2011; Herrero, 2008; Karoui and Blecker, 2011; Mauer et al., 2009; Wang and Sun, 2003; Wu et al., 2008). However, the techniques have their own disadvantages. As an integrated alternative, hyperspectral imaging (HSI) can obtain both spectral and spatial information from the targets (Gowen et al., 2007). As a result, the merits in spectroscopy and computer vision are both reflected in hyperspectral imaging. Furthermore, besides these aggregated advantages from both methods, more benefits are produced. For example, such a system can facilitate acquiring spectra in user-defined areas, where corresponding relationship between spectra and reference values is ensured. Moreover, hyperspectral imaging can also be used to generate chemical maps to show distributions of parameters of interest. However, the rich information in hyperspectral imaging also results in difficulties in data processing, which makes it hard for industrial online applications. To overcome this problem, a simplified version called multispectral imaging (MSI) is available. The difference between the two only lies in the number of bands involved. For HSI, there are normally more than 100 bands, while for MSI, it is usually less than 10 (ElMasry and Sun, 2010). The success of MSI deeply relies on the efficiency of HSI for providing the important wavelengths. A brief comparison of the above-mentioned techniques are summarized in Table 1 (ElMasry and Sun, 2010; Gowen et al., 2007).

In hyperspectral imaging, several choices can be taken to carry out the detection work. These options involve near-infrared HSI, fluorescence HSI, as well as Raman HSI, which provide great flexibility in searching solutions for all sorts of detection problems. In other words, the versatility of hyperspectral imaging has built up its wide applications in food inspection. Although several review papers have been published which however are mainly focused on food quality detection (ElMasry et al., 2011; 2011; Gowen et al., 2007), no paper is available to specifically address the application of HSI to food safety surveillance. Therefore, the objective of this paper is to introduce the principles of hyperspectral imaging and review its applications in different aspects of food safety.

Table 1 Comparison of computer vision (CV), near-infrared spectroscopy (NIRS), multispectral imaging (MSI) and hyperspectral imaging (HSI)

Features	NIRS	CV	MSI	HSI
Spatial information		√	√	√
Spectral information	√		limited	√
Multi-constituent information	√	limited	limited	√
Sensitive to minor components	limited		limited	√
Building chemical images			limited	√
Flexibility of spectral information extraction			limited	√

FUNDAMENTALS OF HYPERSPECTRAL IMAGING (HSI)

The principles of hyperspectral imaging technology include hardware to acquire the images and software to process the images so that useful information from the images can be extracted for food safety analysis and control.

Hyperspectral Imaging System

As described above, a sample can be represented by the combination of its spectra and images through hyperspectral imaging system. Therefore, the principle of hyperspectral imaging can be understood by integrating the theories behind spectroscopy and computer vision. Figure 1 shows the configuration of a typical hyperspectral imaging system.

As shown in Fig. 1, a hyperspectral imaging system consists of three main parts: a light source, a light dispersion device and imaging unit to function as the eye, and decision-making components such as computer hardware and software to function as the brain. The light provided by the light source interacts with the food samples, and the detected portion containing both physical and chemical information of the sample will be dispersed and projected onto a two-dimensional detector array in an imaging spectrograph, which serves the same role as human eyes do. The imaging spectrograph normally covers a wide range of both visible and near-infrared region; however, for human eyes, only three bands (red, green, and blue) are differentiated. The acquired signal will then be transferred into a computer for further processing, including digitization, storage, modeling, and decision-making, in a similar way as the brain works.

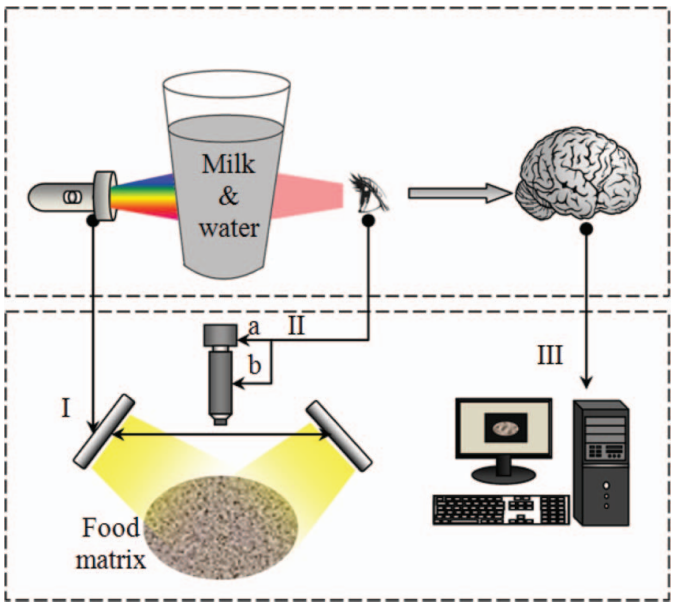

Figure 1 Configuration of a typical hyperspectral imaging system. I: light source; II: spectrograph (a: imaging unit; b: wavelength dispersion apparatus); III: information processor. (color figure available online.)

Detailed description of hyperspectral imaging systems can be found elsewhere (Sun, 2010). However, it should be noted that the wavelength dispersing apparatus sometimes are not necessary especially when developing MSI systems. For example, in multispectral imaging systems based on light-emitting diode (LED) light sources, the different individual wavelength bands can be obtained by switching on the corresponding LED sets (Chevallier et al., 2006; Kulmyrzaev et al., 2008).

Data Structure

The final data acquired by HSI systems are vividly called "hypercube" since they can be illustrated as containing three dimensions with two for spatial coordinates and the other one for spectral values. Accordingly, $I(x, y, \lambda)$ is denoted, where x and y are used to locate the pixels in the image with λ for the wavelength. For the hypercube, if the wavelength λ is fixed, a matrix of spectral responses $I_\lambda(x, y)$ is gained, and the visualization of this matrix produces a gray-level image of the object at the wavelength λ. It should be noted that the collective image (or image stack) for all wavelengths are intrinsically the same as a conventional digital image: they both offer optical perception in a spatial domain. The only difference is in the number of wavebands involved and therefore the amount of characteristic information provided. Particularly, for hypercubes, depending on the wavelength λ concerned, the object of interest may either be apparent to be recognized or merged in the background and noise, resulting in difficulties for identification. Therefore, efficient image analysis methods should be carefully developed and employed to sift useful bands, which will be discussed later. Also, the hypercube can be reconstructed as $I_x(y, \lambda)$ or $I_y(x, \lambda)$. In this way, at a fixed spatial coordinate of either x or y, another matrix indicating the distribution of spectra (covering all the available wavelengths λ) along the other spatial axis y or x can be obtained. In the resultant matrix, a vector is then the spectrum of a pixel. Therefore, the visualized "image" is within the spectrum-spatial domain, and is quite distinctive from the conventional image produced by computer vision. Specifically, a hypercube is the simultaneous display of the successively aligned spectra of their corresponding pixels in the object. The above two ways of understanding a hypercube is by breaking it up into slices, that is, to divide a three-dimensional matrix into a stack of two-dimensional matrix assigned to either spatial-spatial or spatial-spectral coordinate. Alternatively, a hypercube can also be considered as an organized combination of pixel-wise spectra, with the resulting donation as $I_{x,y}(\lambda)$, as is illustrated in Fig. 2.

The above three ways of interpretation of hypercubes correspond to different ways of data acquisition methods, that is, area-scanning imaging (or staring imaging), line-scanning imaging (or pushbroom imaging), as well as point-scanning imaging (or whiskbroom imaging). In area-scanning imaging, the hypercube is obtained by gaining spatial images at all wavelengths in sequence, in line-scanning imaging pixel spectra are acquired line by line, while in point scanning, the spectra are obtained pixel by pixel. Nevertheless, among these three scanning approaches, pushbroom imaging is the most popular one in the food industry due to its readiness for on-line application. Under such a scanning scheme, the object needs to go with a translation stage and pass the field of view of the spectrograph where images are produced. Based on this, only a simple transfer, that is to replace the translation stage with a conveyor in processing line, is necessary for the on-line application.

Data Processing

Hyperspectral imaging system offers massive information about the targets. Consequently, efficient data processing methods are needed to reveal the truth hidden behind these hypercubes (Lorente et al., 2011; Menesatti et al., 2009). In this section, image calibration methods as well as signal processing procedure will be addressed.

Image Correction

The raw images acquired by a HSI system in reflectance, transmittance, or scatter mode, are normally recorded in radiance. However, it is sensitive to the sensors used, which means that the images for the same sample taken under the same condition may differ according to the configurations of the HSI system employed (Yao and Lewis, 2010). To improve the comparability of the image data, radiometric calibration is often performed. Such calibration requires obtaining a dark current image (I_{dark}) and white reference image (I_{white}). After that, the following is

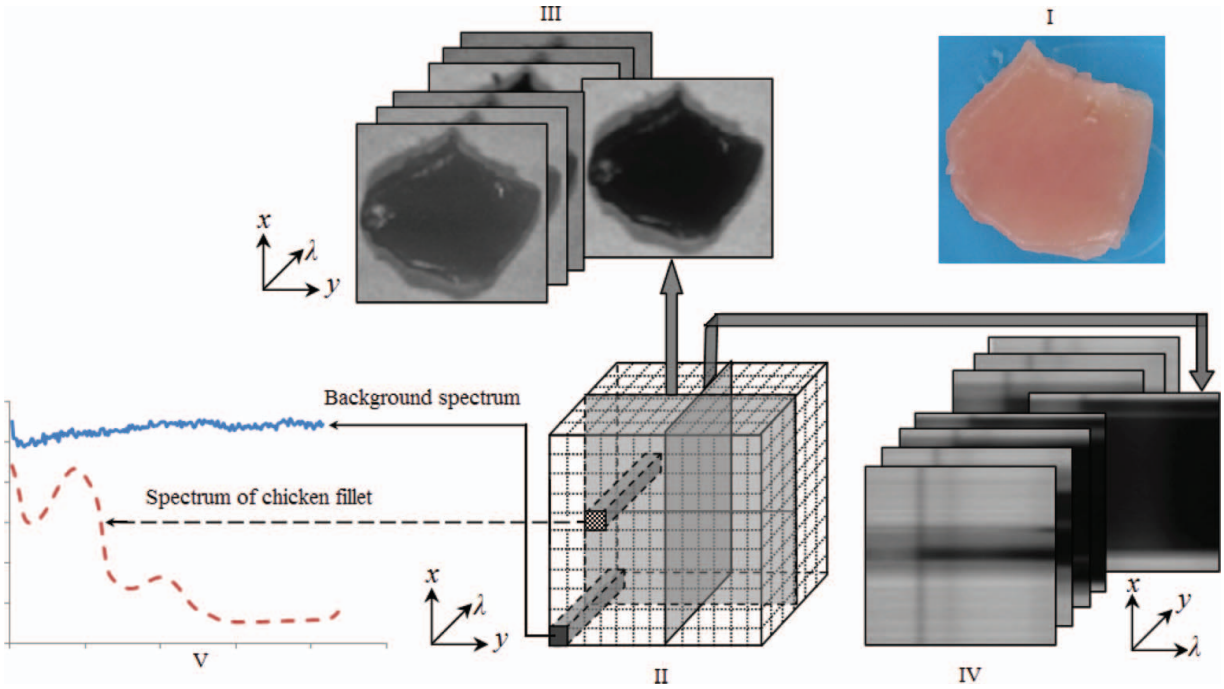

Figure 2 Different ways of understanding a hypercube. I: RGB image of a chicken breast fillet slice; II: the spatial structure of a hypercube; III: front view of the hypercube; IV: side view of the hypercube; V: Spectra of pixels in different portions. (color figure available online.)

utilized for pixel-wise corrections (Lu and Chen, 1998):

$$I_c = (I - I_{dark})/(I_{white} - I_{dark}) \quad (1)$$

where I and I_c are sample images before and after correction. In Eq. (1), the operation in denominator is to eliminate the spatial non-uniformity of the light source and the subtraction in numerator can reduce noise of the system. While as a whole, the percentage generated by division is capable of simplifying subsequent computations. More importantly, spectra from the calibrated images can be interpreted to allocate featured molecular bonds or components.

If no white reference standard is available, the equation below can then be employed, which is also applicable to Raman image correction (Qin et al., 2010):

$$I'_c = I - I_{dark} \quad (2)$$

In addition, Lambert's cosine law is effective in eliminating the effects from surface morphological variations of samples, especially those with spherical shapes (Qin and Lu, 2008). However, it is not necessarily applied in food inspection when using hyperspectral imaging.

For images obtained in fluorescence mode, a different correction method is to be applied due to its different nature from reflectance. To implement such corrections, both reference and dark images are required. Particularly, in collecting reference images, three flat-field materials, that is, premium white inkjet paper, methanol solutions of fluorescein, and rhodamine B are used to account for spectral profiles in blue, green, and red regions, respectively (Kim et al., 2001b). During calibration, a correction factor (CF) is calculated first for every pixel in the image at a certain wavelength, and these factors are then multiplied to individual corresponding pixel of the dark-current-subtracted sample image. The whole procedure is expressed by Kim et al. (2001b) as follows:

$$CF_\lambda = (FR_{ave,\lambda} - FR_{dark,\lambda}) / (FR_{i,\lambda} - F_{dark,\lambda}) \quad (3)$$

$$FS_{ci,\lambda} = CF_\lambda \cdot (FS_{i,\lambda} - F_{dark,\lambda}) \quad (4)$$

where CF_λ represents the correct factors for image at wavelength λ; $FR_{ave,\lambda}$ is the mean of all pixel responses in the reference image at wavelength λ; $F_{dark,\lambda}$ is the dark image at wavelength λ; $FR_{i,\lambda}$ is the intensity of the *i*th pixel in the reference image at wavelength λ; $FS_{c,\lambda}$ and FS_λ are corrected and uncorrected images of the same sample at wavelength λ.

Additionally, $FR_{ave,\lambda}$ should be constantly shifted to acquire radiance-corrected images. However, in case of studies where more interests are focused on the relative changes of the intensities, this step can be skipped.

Data Processing Routines

Because of the special attributes of hypercubes, the analyses can be carried out in two alternative ways: either from perspective of spectral analysis or based on image processing. Nevertheless, appropriate data should be first prepared no

matter which approach is selected. Before spectroscopic analysis, the spectra are first extracted from regions of interest (ROIs), which are mostly determined by thresholding an image at a single waveband or at a ratio and/or difference image. While, for image processing, limited number of images (preferably less than 10) should be chosen from the massive images available to facilitate fast computation. Usually, these images are those at important wavelengths, which require careful sifting. To do this, location of the bands where peaks and valleys occur in the original or preprocessed (mainly, first or second derivatives) spectra offers an option (Shao et al., 2011). To reach the same goal, chemometric methods, such as principal component analysis (PCA) and partial least square regression (PLSR), can be employed where the loadings and importance in projection (VIP) scores can be examined to find out vital wavelengths (ElMasry et al., 2008). Moreover, some other data compression methods (i.e., Fourier transform, singular value decomposition, and so on) can also enhance the capability of HSI for processing more images (Bonnier et al., 2008; Kulmyrzaev et al., 2008). After the data are available, the next task is to establish reliable calibration models. However, before implementing chemometric algorithms, it is necessary to reduce the noise so as to enhance the signal-to-noise ratio. For example, concerning spectral analysis, multiplicative signal correction and standard normal variation can help eliminate light scattering effect arising from physical properties of the samples (i.e., firmness, particle size, etc.), while derivative methods can either suppress baseline shifts or detrend the spectra, so that more details within the spectra can be revealed. In addition, image processing, such as binning, filtering, and so on, can also enhance the quality of data. During model calibration, from the spectral analysis part, it follows the same routines as in spectroscopy, which is shown in Fig. 3. Therefore, it will not be discussed here in detail, and further details can be found elsewhere (Sun, 2009). However, it is worth mentioning that the models built based on whole wavebands should be simplified so that the speed of pixel-wise prediction on a new sample can be substantially accelerated. Such simplification indicates inclusion of only important wavelengths, which can be selected as aforementioned. In terms of image analysis, the methodology applied is similar to what is used in computer

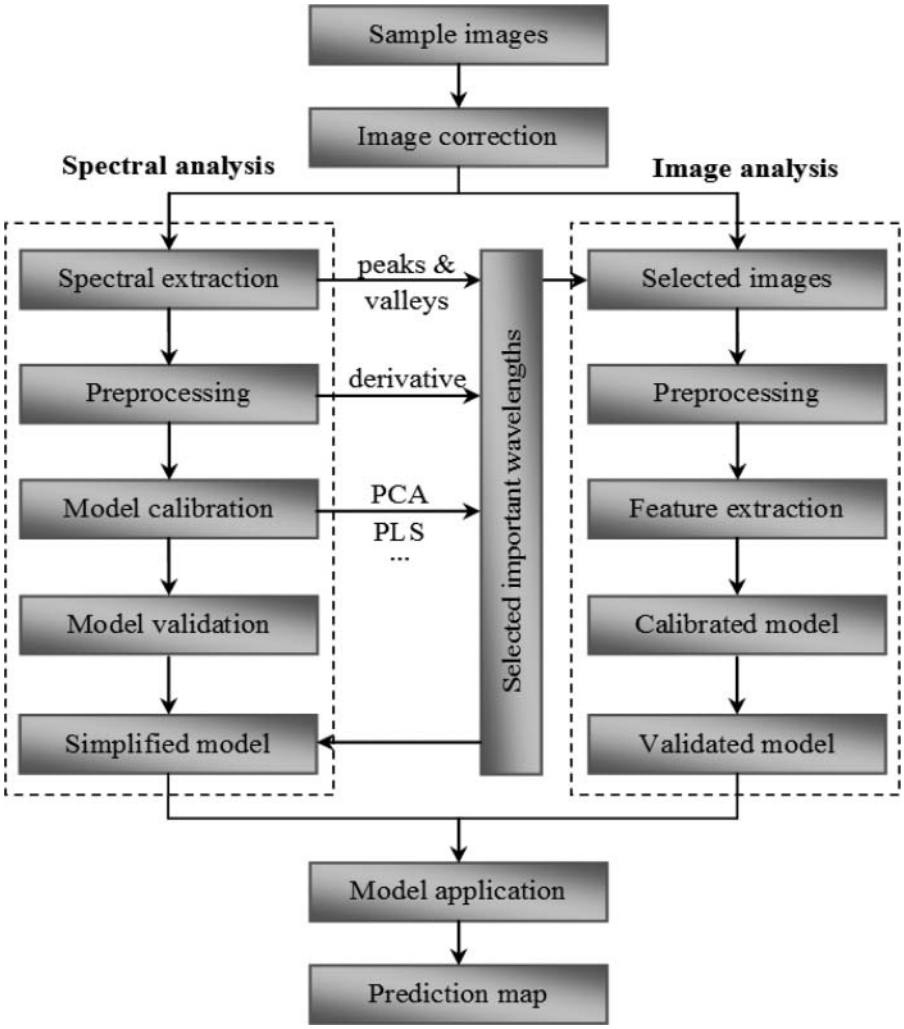

Figure 3 Flow chart of the routine for hyperspectral imaging processing.

vision (Sun, 2008). In such analysis, a critical step is feature extraction, where various features, such as statistical moments and image textures, are to be retained. Thus, by employing spectroscopic or image processing methods, a calibration model can finally be established.

Despite the methodology used, the resulting models fall in two categories, that is, qualitative models and quantitative models. Qualitative models classify the samples into certain groups where each depicts a common trait of the samples included in the group. For doing this, various methods, such as PCA, linear discriminant analysis (LDA), partial least square discriminant analysis (PLS-DA), Fisher's linear discriminant (FLD) method, artificial neural network (ANN), support vector machine (SVM), and fuzzy inference (FI) are available. Quantitative analysis tries to sense the specific physical, chemical, or biological parameters within individual samples. The methods include multiple linear regression (MLR), PLSR, principal component regression (PCR), ANN, and so forth. Finally, the established models need to be checked for adaptability and reliability using cross validation and/or external validation. When verified, they can then be applied on new data pixel by pixel. Consequently, a two-dimensional dataset will be produced where the contents of the samples are clearly visualized. Usually, the prediction map can be improved by employing post-processing methods, taking median filtering for instance. In this way, the information of interest can be made available. Figure 3 gives the whole procedure.

It should be noted that developing a satisfactory calibration model is always a tough task especially when the correlation between target parameters and spectral and image information in hypercubes is not straightforward. For such a reason, different methods in data preprocessing, feature extraction methods and modeling as mentioned above should be investigated, therefore the establishment of useful calibration models can be very time-consuming. However, once a satisfactory model is established, its application then becomes easy and fast, which enables HSI to meet the requirements for rapid, nondestructive, and precise detections in the food industry.

APPLICATIONS

The potential of hyperspectral imaging has been successfully proved in the food industry. Although more studies are conducted in food quality analysis, the application of hyperspectral imaging in food safety inspection and control is increasing, which will be specifically discussed in the following sections.

Physical Contamination and Defects

Fecal contamination on food surface and the presence of foreign materials in food matrices are two main issues in food physical contamination. Meanwhile, the defects of food matrix are always indicators of unsuitability of food for consumption.

Fecal and Ingesta Contamination

Fecal and ingesta contamination can introduce pathogenic microorganisms both in fruits and vegetables and in meats, leading to possible occurrence of food safety incidents.

Fecal Contamination on Fruits and Vegetables. Fecal contamination on apples may result in introduction of pathogenic microorganisms (e.g., *Escherichia coli* O157:H7) into unpasteurized apple juice or cider, which is a potential health threat to the public (Cody et al., 1999). Therefore, they should be refused for further processing. Hyperspectral imaging offers a solution for this through non-destructive measurement of feces on apples. However, when applying it, one should consider some difficulties. One of them lies in the fact that apple features of both appearance and components vary among different cultivars, and even among individuals of the same cultivar due to different environment and growth stages. These variations are of great concern, because they may affect the successful recognition of feces on apples, especially for "Red Delicious," which are more variegated. To eliminate such influence, one possible solution is to pick up wavelengths that are not sensitive to the variations. Kim et al. (2001a) showed that the image in the far-red band (specifically, 800 nm) depicted little or no difference in sun-exposed and shaded surface of Red Delicious when a hyperspectral reflectance imaging system was applied, however, one problem associated with this approach is that the classification accuracy or sensitivity sometimes cannot be guaranteed since only the thick feces could be observed and easily identified in such images, while the thin layers normally appear problematic for detection when one band is used (Kim et al., 2002a). Other choices may include employment of chemometric algorithms and multivariate data analysis. For instance, principal component analysis transforms dataset into sequence of principal components (PCs) where the first several components can be used to represent the overwhelming majority of the information contained in the original data. Interestingly, PCs usually can illustrate main features present in the images (Kim et al., 2002a; 2002b; 2004b). Therefore, by checking these PCs, one may find a certain PC that wears the contaminants but suppresses discrepancies for other information within apples. Thereupon, the impact from apple variation is eradicated. Meanwhile, application of uniform power transformation as well as second difference can also reach similar performance (Lefcourt et al., 2005a; 2005c; Lefcout and Kim, 2006; Mehl et al., 2004).

Actually, the methods mentioned above are not only effective in reducing uninterested information (noise in this case), but also powerful for achieving good classification of normal and contaminated apple skins. However, as mentioned above, processing images in individual characteristic band is normally insufficient because of the complex background involved as well as the intensity similarity between apple edges and feces in the images (Kim et al., 2002a; Lefcout et al., 2006). Therefore, several algebraic operations, that is, subtraction, division, and their combinative manipulation on selected wavelengths, were developed (Lefcout et al., 2006). Among these, in

Table 2 Detection of faecal contamination on fruits and vegetables using hyperspectral imaging

Products	Mode	Methods	References
Apple	Reflectance and fluorescence	Band ratio and thresholding	(Kim et al., 2001a)
Apple	Reflectance	PCA and thresholding	(Kim et al., 2002a)
Apple	Fluorescence	PCA, band ratio and thresholding	(Kim et al., 2002b)
Apple	Fluorescence	Thresholding	(Lefcourt et al., 2005a)
Apple	Fluorescence	Thresholding or edge detection	(Lefcourt et al., 2005b)
Apple	Fluorescence	Uniform power transformation	(Lefcout and Kim, 2006)
Apple	Reflectance & fluorescence	Band difference Band ratio	(Lefcout et al., 2006)
Apple	Reflectance	Band ratio, second difference and principal component analysis	(Liu et al., 2007)
Apple	Fluorescence	Separation algorithms based on peak shift and shoulder curve	(Yang et al., 2011; 2012)
Cantaloupe	Fluorescence	Band ratio and PCA	(Vargas et al., 2004; 2005)
Strawberry	Fluorescence	Band ratio and PCA	(Vargas et al., 2004)
Lettuce and spinach	Fluorescence	Band ratio, thresholding and median filtering	(Yang et al., 2010)

detection of feces, quotient generally outperforms simple difference when two chosen wavelengths are used (Liu et al., 2003). Moreover, it is always suggested that their combination should be investigated to improve the classification accuracy by introducing a new band (Lawrence et al., 2006). However, this was sometimes wavelength-dependent, and one of the exceptions occurred when Liu et al.(2007) obtained the best classification by using a two-band ratio, that is, R_{725}/R_{811}, where the quotient of difference utilizing three bands yielded less contrast than the two-band ratio method. Differently, another recently-developed simple algorithm based on peak shifts and shoulder curves was employed when a multispectral fluorescence imaging system was investigated in the red and the far red region (Yang et al., 2011; 2012).

Not limited in apples, some of the aforementioned methods were also used to detect feces on cantaloupes (Vargas et al., 2004; 2005), strawberries (Vargas et al., 2004), lettuce, and spinach (Yang et al., 2010). The above-mentioned studies are summarized in Table 2.

Feces and/or Ingesta on Meat. Ensuring meat quality and safety is very important for the meat industry (Desmond et al., 2000; McDonald and Sun, 2001; McDonald et al., 2001). Similar to the case of apples, fecal or ingesta contamination of poultry meat is also of great concern and the US government mandates zero-tolerance policy for inspection (Lawrence et al., 2003). Statistically speaking, uncontaminated poultry carcasses can be modeled by a Gaussian distribution, whereas contaminated materials are of non-Gaussian properties (Yoon et al., 2007). This finding signifies possible discrimination of the two. As a powerful tool, hyperspectral imaging was initially demonstrated to be effective for identification of feces on two chicken carcasses (Heitschmidt et al., 1998). However, better discrimination required inclusion of more chicken and varieties of feeds, which were expected to cover a board range of variations so that the model subsequently built, could be representative and adaptive. Later, Lawrence et al. (2001) suggested evaluation of the effect of scalding chicken carcasses on classification accuracy. Thereafter, most of the research considered these factors. On one hand, for instance, Windham et al. (2002) fed 300 birds with different feeds, including corn, milo, and wheat, and after the broilers were killed and excised, feces and ingesta were collected from their duodenum, ceca, as well as colon and crop, respectively. During image processing, usage of two bands (565 and 517 nm) resulted in an overall accuracy of 90.61%, which was good but poorer than that gained in some later studies (Lawrence et al., 2006; 2003; Park et al., 2006). This disparity may emanate from the different sizes of sample sets, but more probably lies in the variations within feces and ingesta due to different feeding. Windham et al. (2002) also optimized selection of wavelengths, and achieved the best identification on image at 458 nm if only one band was used, at 576 and 529 nm for two-band ratio, and with added 616 nm for the three-band algorithm. Despite this discovery, the two bands, that is, 565 and 517 nm are more prevalently employed. Using these two wavelengths, many researchers successfully categorized carcass images into two groups, clean and contaminated, and the result was even checked in pixel-wise to account for light contamination, as an elucidation of micro-scale precise detection (Windham et al., 2005; 2005). Not only capable of identifying tainted spots (big or tiny) in carcasses; moreover, hyperspectral imaging system in tandem with spectral angle mapper (SAM) was reported to be sensitive enough for determining the type of contaminants, which may provide knowledge about source of contamination, thus facilitating decision-making for necessary adjustments at critical control points (Park et al., 2004b; 2007). On the other hand, in terms of studies on expatiating washing effect, Lawrence et al. (2006) designed an experiment where two exposure times and two washing times were included, and the result illustrated that with longer exposure time, more fecal strains could be detected, while washing time did not significantly affect the classification. However, strains are not considered as hazards, therefore, their identification would turn out to be false positive for fecal detection systems. To avoid this, Lawrence et al. (2006) suggested the addition of a third wavelength.

Table 3 Applications of hyperspectral imaging in detection of fecal contamination on chicken carcasses, sorted in chronological order

Methods	Accuracy	Reference
Principal component analysis, spectral angle mapper and Mahalanobis distance classifier	–	(Heitschmidt et al., 1998)
Band ratio, histogram stretching and thresholding	97.3%–100%	(Lawrence et al., 2001)
Band ratio and thresholding	96%	(Park et al., 2002)
Band ratio and thresholding	100%	(Windham et al., 2002)
Band ratio and thresholding	92.4%–98%	(Park et al., 2004a)
Spectral angle mapping	90.13%	(Park et al., 2004b)
Band ratio, thresholding and median filtering	92.5%–96.9%	(Park et al., 2005)
Decision tree	100% 53%–72%[a]	(Windham et al., 2005)
Band ratio and thresholding	94%–100% 35%–74%[a]	(Windham et al., 2005)
Band ratio and thresholding	98.2%	(Lawrence et al., 2006)
Band ratio and decision tree	>99%	(Heitschmidt et al., 2007)
Band ratio and thresholding	96.40%	(Park et al., 2006)
Band ratio, thresholding and filtering	–	(Park et al., 2007a)
Spectral angle mapping	90.13%	(Park et al., 2007b)
Statistical model-based thresholding	98.18%	(Yoon et al., 2007)
Band ratio and thresholding	–	(Kise et al., 2008)
Co-occurrence matrix based textural analysis	–	(Park et al., 2008)
Band ratio and thresholding	–	(Park et al., 2011a)
Binning, cuticle removal filter, median filter, and morphological analysis	∼91%	(Park et al., 2011b)

[a]: percentage of the faecal ground truth detected

It is always in the interest of the food industry to develop online systems for fecal detection on broiler carcasses. However, hyperspectral imaging systems usually produce data of huge size, which is not favored for real-time application, especially when advanced hardware and software are not available. Therefore, multispectral imaging systems were developed instead to accomplish this task (Lawrence et al., 2002; Park et al., 2004a; 2002). After preliminary investigations, several adjustments of both hardware and software were conducted. For example, the multispectral imaging system was modified by changing the lights, camera, and spectrograph to create better configurations for measurements (Heitschmidt et al., 2007). And later, unified modeling language (UML) was used to develop user-defined and specialized software for real-time detection (Park et al., 2007). Also, efforts were devoted to optimize data processing procedures to find an optimum trade-off for higher precision and less false alarming (Park et al., 2011). Detection results all demonstrated the effectiveness of these systems for identifying feces on poultry surfaces in spite of the harsh environment involved. Furthermore, in more recent studies of in-plant real-time detection, hyperspectral imaging system successfully identified fecal spots on the carcasses at a high-speed processing line (140 birds per minute), and the detectable feces could be as little as 10 mg (Park et al., 2011; 2011). Besides, a prototype for a hand-held multispectral imaging system with light-emitting diode (LED) lights was also developed (Kise et al., 2008).

Instead of inspecting the surface of carcasses discussed above, some researchers looked into the visceral cavity of chicken, the detection of which is also quite important but simultaneously of more challenge because more spectral profiles are involved in the inner side of the chicken carcasses. Park et al. (2005) compared spectra of various sources and applied different thresholds as well as filters on the ratio images of at 565 and 517 nm, and gained an accuracy of as high as 96.9% though a few false positives were noticed. To reduce the occurrence of these alarming, textural analysis utilizing co-occurrence matrix was employed before and after band ratio operation (Park et al., 2008). This method was proved to be effective in eliminating false positives, and meanwhile it could also enhance the accuracy especially when conducted after image ratio.

The above studies dealing with fecal contamination detection on chicken carcasses by HSI are listed in Table 3. In addition, feces on pork was also successfully detected by a multispectral laser-induced fluorescence imaging system (Kim et al., 2003).

Detection of Foreign Materials

The presence of foreign substances in food commodities should be eliminated because they are hazardous to consumers. Yoon et al. (2006) investigated the feasibility of using hyperspectral imaging on detecting bone fragments in boneless chicken fillets, and found that all the bones inserted in the meat could be recognized in transmittance mode given that the fillets were examined on both sides, and reflectance analysis enabled elimination of false positives. Based on the results, samples were later categorized into two classes, namely, with and without bones, under both transmittance and reflectance modes (Yoon et al., 2008a). The two resultant prediction maps were then fused by subtraction for eventual judgments. In another fusion, the prediction map was first produced by analyzing the transmittance images and the recognized candidate areas were then further checked to determine whether they are false alarming or not according to specific reflectance responses (Yoon et al., 2008b).

Besides bone fragments, other foreign materials were also monitored. For blueberries, Tusta et al. (2006) examined twigs, worms, stones, and hairs using microscopic Vis/NIR imaging, while stems and leaves were measured by Sugiyama et al. (2010). Moreover, Jiang et al. (2007) classified walnut shell out of pulp, and Bhuvaneswari et al. (2011) established quantitative PLS models for assessing insect fragments in semolina.

Detection of Defects

Defects in food usually indicate that food is unsuitable for consumption. The defects in fruits and vegetables include bruises, chilling injuries, canker and rottenness. While septicemia/toxemia, inflammatory process, and skin tumors are some examples for abnormality in meat.

Detection of Defects in Fruits and Vegetables. The presence of defects in fruits and vegetables usually indicates possible invasion and dwelling of pathogenic microbes in the flawed portions of the commodities appearing as symptoms such as bruises or lesions (Kim et al., 2001a; Mehl et al., 2001). These defects can undergo a fast deterioration process, thus pose great threats to human beings, especially when they are mistakenly used for producing cider and beverage. The applications of HSI for detecting defects in fruits and vegetables are inventoried in Table 4. When hyperspectral imaging is used to inspect defects, two most popular commodities studied are apple and cucumber for bruises and chilling injuries, respectively. For determination of bruises in apples, Lu et al. (1999) first tried on three cultivars and found that the band between 700 and 900 nm (in NIR region) was most useful for implementing such a task. According to this result, Lu (2003) later employed a HSI system in 900–1700 nm to study its potential for predicting bruises of different storage time after bruising. By integrating PCA and minimum noise fraction transform (MNF), he found that for Red Delicious apples, the highest classification accuracy was gained for one day after bruises occurrence (88.1%). Additionally, there was a general decreasing trend in accuracy with the increase of storage time. However, for Golden Delicious cultivar, the accuracy generally increased with the storage time, with the highest happening on Day 47 (93.8%). This phenomenon suggested that the variation among cultivars affected the detection greatly. As a result, most of the studies later focused only on one variety each time. One example was for recognizing bruises on Golden Delicious apples, where Xing et al. (2007) used both supervised and unsupervised classification methods. They found PLSDA had more potential as compared with PCA, since the prediction map produced was free from effects of sample surface curvatures. Furthermore, it was suggested that the prevalent false positives from stem-end and calyx could be eliminated if their spectra were carefully considered. In another investigation which was devoted to early detection of bruises on "McIntosh" apples, ElMasry et al. (2008) found that HSI could sense bruises as early as 1 h after bruising. To enhance the performance, median filter coupled with dilation and erosion analysis was performed to remove false alarms that had similar spectral profiles as the bruises. Alternatively, pertaining to the specific case of bruises whose shapes are always smoothly circular, some shape calculation can be conducted to remove small areas and elongated regions and finally to identify the true positives on the preliminary prediction map (Xing et al., 2005). Instead of simply applying the thresholding method on selected or synthesized images, some authors turned to elucidate the inspection in image

Table 4 Applications of hyperspectral imaging for defect detection in fruits and vegetables, sorted by product categories and defects

Products	Detection of	Method	Accuracy	References
Apple	Bitter pit lesion	PLSDA	–	(Nicolaï et al., 2006)
Apple	Bitter pit, black rot, decay and scald	ANN	87.6%–95.4%	(Ariana et al., 2006)
Apple	Black pox, bruise, rot, and sooty blotch	BR	99.5%	(Kim et al., 2007)
Apple	Black pox, bruises, side rots, molds and scabs	SD, PCA, and T	–	(Mehl et al., 2004)
Apple	Brown decayed spots, open wounds and rot	BR	92.42%	(Lee et al., 2008)
Apple	Bruises	PCA; PLSDA	86.33%; 2.3%	(Xing et al., 2007)
Apple	Bruises	T	–	(ElMasry et al., 2008)
Apple	Bruises	PCA and MT	86%	(Xing et al., 2005)
Apple	Bruises	PCA and IPS	77.5%–100%	(Xing and De Baerdemaeker, 2005)
Apple	Bruises	PCA		(Lu et al., 1999)
Apple	Bruises	PCA, MNF, and T	62%–88%	(Lu, 2003)
Citrus	Canker	SID	96.2%	(Qin et al., 2009)
Citrus	Rottenness	ANN; CART	99.31%; 98.30%	(Gómez-Sanchis et al., 2012)
Cucumbers	Bruises	BR, BD, PCA, and T	75%–95%	(Ariana et al., 2006)
Cucumbers	Chilling injury	PCA-FLD	91%	(Cheng et al., 2004)
Cucumbers	Chilling injury	BR and PCA	>90%	(Liu et al., 2005; 2006)
Mushroom	Bruises	PCA	79%–100%	(Gowen et al., 2008)
Onion	Sour skin disease	–	–	(Wang et al., 2009)
Strawberries	Bruise	LDA, ND, and ANN	Up to 100%	(Nagata et al., 2006)

PLSDA: partial least square discriminant analysis; ANN: artificial neutral network; BR: band ratio algorithm; SD: second difference analysis; PCA: principal component analysis; T: thresholding; MT: moments thresholding; IPS: an image processing scheme; MNF: minimum noise fraction transform; SID: spectral information divergence; CART: classification and regression tree; BD: band difference; FLD: Fisher linear discriminant; LDA: linear discriminant analysis; ND: normalized difference.

processing regimes. For example, by assuming that the occurrence of bruises, stem-end, and calyx could result in deformation of apple shape, Xing and De Baerdemaeker (2005) analyzed the characteristics of contours for sound, bruised apples and their stem-end and calyxes. Based on the results, they developed a successful scheme to discriminate bruised portions from others. Moreover, in terms of bruise inspection, some other fruits and vegetables were also studied including cucumber (Ariana et al., 2006), strawberry (Nagata et al., 2006), and mushroom (Gowen et al., 2008). Among these studies, PCA were frequently used to extract features or to reduce data size. However, band difference was frequently suggested for future application because of its simplicity and equivalent performance to PCA.

There is not much literature available as in bruise detection with regard to chilling determination. Nevertheless, the feasibility of HSI is still proved for this application. By employing band ratio or PCA, accuracy of over 90% could be achieved, and the identified wavelengths were useful for future development of MSI (Liu et al., 2005; 2006). Another innovative method utilized in this area is the combined algorithm of PCA-FLD (Cheng et al., 2004). This integration is not a simple sequential use of the methods, but based on a developed equation where both functions of PCA and FLD were reflected. A few other papers found on inspection of specific defects on other produces include sour skin in onions (Wang et al., 2009), and canker and rottenness in citrus (Gómez-Sanchis et al., 2012; Qin et al., 2009).

Apart from the single defect detecting studies introduced above as well as additional bitter pit lesion determination on apples (Nicolaï et al., 2006), some studies dealt with classification of comprehensive defects. Mehl et al. (2004) employed an asymmetric second difference method to detect side rot, bruise, scab, flyspecks, etc., on four varieties of apples, and the result was excellent, showing distinctive separation of normal and defective parts regardless of discrepancy in cultivar and color. Kim et al. (2007) discovered that a simple classification was sufficient to reach very good result if mean and coefficients of variation of the ratio values were taken as input, and by doing this, an accuracy as high as 99.5% was gained and the false positive rate was low (2%). The effectiveness of ratio algorithm was also demonstrated by Lee et al. (2008) when they determined open wounds, rot and brown decayed spots on Fuji apples. There is another research utilizing both reflectance and fluorescence imaging modes. Ariana and others (2006) built ANN models to categorize apples into either two groups (normal and defect) or multi classes (normal, bitter pit, block rot, decay, soft scald, and superficial scald tissues). The results indicated that the detection of defects on Honeycrisp apples required the two modes to work together for satisfactory performance. While for Redcort and Red Delicious, either mode could be competent.

Chicken with Pathological Diseases. Systemically diseased chicken refer to the chicken infected with septicemia/toxemia or inflammatory process where pathogenic microbes and toxic wastes as well as inadequate absorption of yolk sac are to be blamed (Chao et al., 2007b; Yang et al., 2005). Unwholesomeness of chicken also includes the symptom of tumors, and thickened skin areas usually with ulcerous lesions in the middle (Calnek et al., 1991). For safety concerns, these abnormalities are mandated to be completely removed from processing lines and isolated from the normal chicken. To achieve this goal, hyperspectral imaging has been investigated to test the wholesomeness condition of broilers. The discrepancies within spectra of wholesome and systemically diseased chicken are prominent at feature wavelengths (Lu and Chen, 1998), and this fact formed the basis for the identification of unwholesome from wholesome chicken. However, to use these discrepancies effectively, one should carefully consider some factors.

First, the choices of light sources can lead to complexity of the whole detecting system. For example, quartz–tungsten–halogen (QTH) light requires more manipulation gain from the camera than light-emitting-diode (LED) illumination (Yang et al., 2006). More importantly, QTH produces lower intensities at short wavelengths that are closely related with myoglobin, and such weakness would result in overlapping of envelops of the standard deviations of the spectra of wholesome and unwholesome chickens. Consequently, more difficulties may arise in subsequent classification algorithm design.

Secondly, it has been demonstrated that the position and size of ROIs can influence the result (Chao, 2010; 2008). Symptoms of septicemia and toxemia can mostly be found in the breast and lower abdomen of chicken, and these areas therefore can be considered as potential ROIs (Yang et al., 2005). To locate them in the images, some authors identified four corners and connected them with straight lines or using the boundaries of chicken, and the remaining parts of carcass images were assigned as the uppers and lowers, respectively (Yang et al., 2006). Among these three ROIs, which allocated different positions of the chicken, the middle one was expected to be the best part for producing satisfactory outcomes. To illustrate the influence of ROI size, Chao et al. (2007b) defined an area whose border consisted of an upper line and a lower one and the chicken boundary between them. Within this area, they adjusted the area by positioning two other lines defined as percentage of the distance between the upper and lower lines, and found the range of 45%–55% gave the largest spectral difference. However, later, 50%–60% was reported as the optimal option (Chao et al., 2007a), and most recently, Chao et al. (2010) preferred 40%–60% in an in-plant and on-line evaluation. Though no big difference was observed, this phenomenon indicated the need for careful selection of ROIs in future work.

Thirdly, the performance of identification relies on the discrimination analysis methods used or how they are used as well. In the case of systemically diseased and inflammatory chicken inspection, most researchers chose differentiation based on fuzzy logic, with some others turned to classification and regression trees (CART) decision tree statistic algorithm. However, whichever method is to be used, there is a need to find appropriate parameters to feed these algorithms, and the appropriate parameters may be the average intensity value at each waveband before and after normalization, the average ratio of images at two bands before and after normalization, the average

principal component values, the statistical standard deviations, or probably their combinations. However, most of the time, the simple average of intensities in the feature bands would be sufficient enough to produce satisfactory results when predicting the wholesomeness conditions of chicken (Chao et al., 2007a; Yang et al., 2005; 2006). In addition, average values at feature wavelengths, together with band ratios at key wavelength pairs, were used for online applications (Chao et al., 2010).

The detection of the above-mentioned diseases is summarized in Table 5. However, it is more difficult to detect tumors than Septox in reflectance mode because of the subtle differences located in the spectral responses of normal and tumor chicken (Lu and Chen, 1998). Nevertheless, by proper feature selection, it is still effective to employ the hyperspectral imaging system for such a task. For example, Chao et al. (2002) applied PCA on the hypercubes obtained and found tumors appeared in the blue and green bands. After creating a feature image by the ratio of three bands, they calculated four statistical moments (later translated into three features) as inputs for a fuzzy interference system. Chao et al. (2002) finally found that combinative

Table 5 Detection of diseased chicken carcasses based on hyperspectral imaging (sorted by diseases and year of publication)

Detecting	Mode	Feature extraction and classification methods	References
Septox[a]	Reflection	Methods of PCA and ROI were used for classification of septicemic and inflammatory process chickens, respectively. Their combinative use together with decision tree realized the separation of different types of diseased as well as normal chickens.	(Yang et al., 2005)
Septox	Reflection	Features were selected based on some wavelengths and PCA and these features were taken as inputs for a decision tree algorithm for discrimination	(Yang et al., 2005; Yang et al., 2006)
Septox	Reflection	Fuzzy logic was developed based on the ratio images	(Yang et al., 2006)
Septox	Reflection	Based on the wavelengths selected from difference spectrum, discrimination was accomplished using fuzzy logic	(Chao et al., 2007a; 2007b)
Septox	Reflection	For the online application, size and position of ROIs and ratios of key wavelengths were optimized. Fuzzy logic was employed to tell the wholesome from the unwholesome chicken.	(Chao et al., 2008)
Tumor	Reflection	Statistical moments were extracted from defined ROIs in ratio images and fuzzy rules based on the values of features were employed for classification.	(Chao et al., 2002)
Tumor	Fluorescence	The first two principal components were used to represent the data, and support vector machine was employed for discrimination.	(Fletcher and Kong, 2003)
Tumor	Fluorescence	Sensor fusion was employed. Features for spectral classification were chosen according to intensity. The ratio of major axis to minor axis and the number of pixels in candidate areas of tumors were used for spatial discrimination.	(Kim et al., 2004a)
Tumor	Fluorescence	Average of images around wavelengths of interest and their algebraic operations were taken as inputs for fuzzy interference.	(Kong et al., 2004)
Tumor	Fluorescence	Band ratio was selected by minimizing the overlapping area of probability density function of normal skin and tumor, and Radial basis probabilistic neural network was then applied for classification.	(Kim et al., 2006)
Tumor	Fluorescence	Three feature selection methods, that is recursive divergence, exhaustive search and canonical analysis were compared, where support vector machine was used for classification.	(Du et al., 2007)
Tumor	Reflection	Modified branch and bound algorithm and K-nearest neighbor classifier were utilized for feature selection and discrimination	(Nakariyakul and Casasent, 2007)
Tumor	Reflection and fluorescence	Classification of tumors and normal skins was accomplished using features extracted by principal component analysis, discrete wavelet transform, and kernel discrimination, respectively. By a product rule, these results were combined for a better performance.	(Xu et al., 2007)
Tumor	Reflection	Adaptive brand and bound algorithm was used to select wavelengths and support vector machine was employed to recognize the tumors.	(Nakariyakul and Casasent, 2009)

[a]: a condition of either septicemia or toxemia.

use of all the features resulted in the optimal and satisfactory classification. Later, more feature selection methods as well as qualitative approaches were applied to enhance the accuracy. Branch and bound (BB) is one of the effective feature selection methods (Narendra, 1977), and based on this, both modified and adaptive branch and bound (MBB and ABB) were developed (Nakariyakul and Casasent, 2007; 2009). Other feature selection methods, including discrete wavelet analysis, kernel discrimination analysis, and high dimensional generalized discrimination, were also found (Kong et al., 2004; Nakariyakul and Casasent, 2009; Xu et al., 2007). In terms of classification approaches, various linear and nonlinear technologies were utilized, including simple linear classifier, support vector machine, as well as k-nearest neighbor classifier. Besides these, of more interest is the idea of data fusion, either integrative interpretation of specific features or combinative use of multivariate data analysis methods. According to the nature of tumors, which can be divided into two parts, that is, lesion and surrounded thickened skin, Nakariyakul and Casasent (2007) selected features and established classification models for these two parts separately, and the two resulting images were then fused via a fusion rule. Instead of decomposing diseased spots, Xu et al. (2007) extracted different tumor features by using three different methods individually, and the final decision on wholesomeness was also made after information integration through product rules. The similarity with these two examples lies in that when individual feature was used, the solution for a comparatively difficult problem is normally unsatisfactory, but when they are used together, better results can be achieved and due to that more comprehensive and useful information is available for accurate analyses. Besides, in order to gain good performance, another choice is worth trying, that is, to employ new configurations of the system, which may give prominence to the targets. As in the case of tumor detection by hyperspectral fluorescence imaging, the fluorescence intensities of normal skin are generally higher than those of tumor tissues. Working in this mode, classification accuracy of 96% and 90.6% were obtained using support vector machine with features selected by PCA and recursive divergence, respectively (Du et al., 2007; Fletcher and Kong, 2003), which were higher than those when reflectance was applied (Nakariyakul and Casasent, 2009). Moreover, since the spectra resulting from fluorescence lighting are of broad peaks, some researchers focused on these bands and computed the average (Kong et al., 2004), difference (Kim et al., 2004a; Kong et al., 2004) as well as maximum (Kim et al., 2004a) and utilized them as inputs for fuzzy interference. Another way of choosing features was done based on the estimated probability density function of both wholesome and tumor pixels. When the wavelength pairs were generated by this method and classified by radial basis probabilistic neural network, the classification rate was as high as 98.2% (Kim et al., 2006).

Chemical Contamination

Chemical contamination involves a wide range of variations. However, in terms of detection by hyperspectral imaging, only a few were investigated. In the following sections, the application of hyperspectral imaging in detection of melamine and pesticide residue will be discussed.

Adulteration of Melamine

The safety-related food adulteration refers to the intentional addition of hazards into food. Among various examples, melamine is the most notorious due to the outbreak of milk powder scandal in China back in 2008 (Wu et al., 2009). The traditional Kjeldahl and Dumas method failed to detect melamine, because it only measures total nitrogen, which cannot reflect the content of melamine. Instead, both Raman and near-infrared hyperspectral imaging were investigated for their competence. Based on the study of Raman spectra, Liu et al. (2009) found a prominent peak for melamine at 670 cm^{-1} and sample images at this band were subsequently analyzed, where melamine was successfully discriminated from wheat flour. After the pilot study, Raman chemical imaging was then fused with NIR chemical imaging to classify melamine from skim milk powder, and eventually a better accuracy was obtained than when the two technologies were utilized individually (Priore et al., 2009). The above experiments were all carried out in microscopic scale. However, in the food industry, it is always preferable to work in macro-level to acquire sweeping surface information about the food matrix as well as to adapt to the fast operations on food production line. Pirore et al. (2009) found that melamine can be precisely classified and well predicted with macroscopic Raman and NIR chemical imaging, respectively. However, more homogeneous samples were suggested for improvement of the limit of quantification. Other studies focusing on melamine detection in macroscopic scale include two investigations using point scanning mode instead of area scanning as adopted by Priore et al. (2009). In one work, Qin et al. (2010) depicted the setup of a whiskbroom imaging system in details and demonstrated its calibration, and finally, as an example, its effectiveness in detecting and visualizing targets of low concentration (evenly distributed melamine in dry milk powder in this case) was demonstrated, and the prediction map is shown in Fig. 4. In another work, on the same platform, besides screening melamine, another algorithm named self-modeling mixture analysis (SMMA) was implemented during analyzing ammonium sulfate, dicyandiamide, and urea in milk powder (Chao et al., 2011). The extracted spectra of the three adulterants were very similar to what were obtained by scanning the pure substances especially when the contaminants took higher proportion in the mixture. This technique may provide an innovative alternative for improving the accuracy amid both qualitative and quantitative assay of certain components in complex biological materials.

Pesticide Residues

The accumulative pesticide residues in the human body through eating contaminated food can lead to chronic diseases, such as cardiovascular disease, diabetes, cancer, and so on (Bolognesi and Morasso, 2000). Starting from the point of

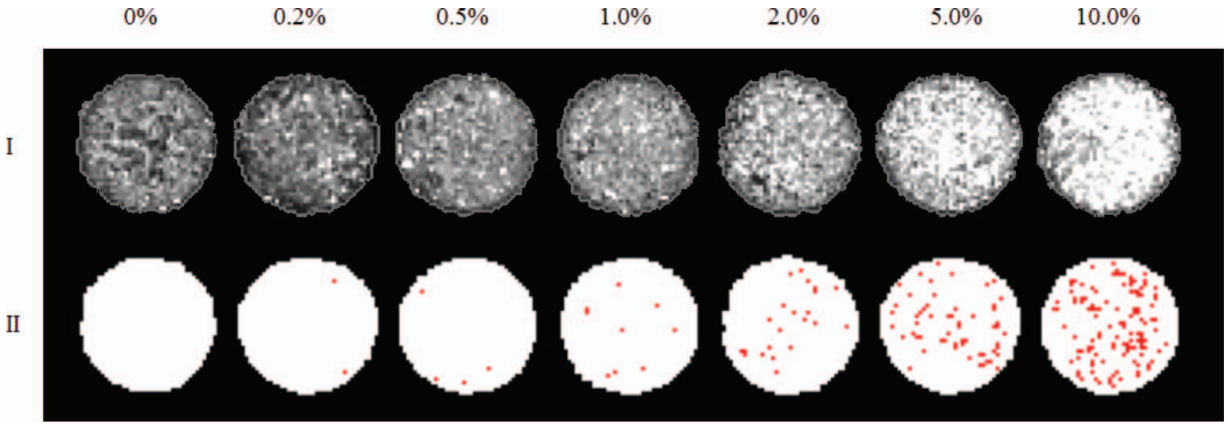

Figure 4 Raman images (I) and prediction map (II) of milk powder adulterated with different concentrations of melamine (Qin et al., 2010). Raman images shown were acquired at 675.4 cm^{-1}. The red dots in the prediction map indicate the presence of melamine in milk powder. (color figure available online.)

view of image processing, Xue et al. (2008) studied the feasibility of detecting methomyl on navel oranges by HSI. After applying principal component analysis to the images acquired, where 4 PCs contributed 99.18% of the total information, Xue et al. (2008) found that the third PC gave the best discrimination result. They also checked the loadings for individual PCs and identified important wavelengths in expectation of developing multispectral imaging system for online inspection in the future. Using the same system (but with different lighting system) on the same product, quantitative analysis of concentration of dichlorvos was studied through spectroscopic and chemometric assays (Li et al., 2010). In the research (Li et al., 2010), satisfactory PLS models were established based on both full and selected wavelengths, but at the cost of model simplicity (at least 12 PCs were required). Another interesting setup employed during screening methamidophos in/on spinach leaves is a hyperspectral fluorescence imaging system with an excitation-emission matrix (Tsuta et al., 2009). In this system, traditional light source was replaced by a spectral illuminator. This could be taken as amalgamation of many monochromatic light sources, among which only one was valid during each scan. Therefore, the resultant image for a sample contained four dimensional data, with the first three being the same in definition as traditional hypercubes produced by area scanning HSI system, and the fourth dimension being the excitation wavelengths. Using such apparatus, Tsuta et al. (2009) demonstrated that SVM was superior to linear discrimination analysis because it provided higher classification rate and fewer false alarms.

Microbiological Contamination

Currently, the detection of microorganisms in food relies heavily on culture and colony counting methods, which are commonly recognized as standard approaches. However, these techniques are destructive, laborious, and time-consuming. Instead, hyperspectral imaging has been explored for determination of microorganisms, including bacteria, fungi, and parasites, in a fast and precise way.

Bacterial Determination

Bacterial pathogens are the most confronted culprits for food poisoning caused by microbial hazards. Therefore, it is substantially important to know whether the meat to be eaten is still at acceptable level of bacterial loads or not, or whether undesired pathogens are present. Due to these concerns, on one hand, research for freshness/spoilage evaluation has been actively conducted, mainly focusing on meat and meat products. On the other hand, efforts have also been devoted to both qualify and quantify bacterial loads on a wide range of food matrices.

In spoilage study of beef, a hyperspectral imaging system in scattering mode was employed by Peng et al. (2011), who accounted for the scattering images using Lorentzian distribution function, with two parameters being subsequently used as inputs for calibration models. They finally found that the multiplication of the two parameters helped give the best prediction. On the same equipment, the total viable count in fresh pork was also investigated. Wang et al. (2010) compared different modeling strategies, among which LS-SVM performed best, with the coefficients of determination as high as 0.9426. This model is good if considering that it was built on a small sample set where the range of reference values was limited. Also based on LS-SVM, Wang et al. (2011) built a model from eight selected wavelengths and a similar good result was gained ($R^2 = 0.9236$). For another batch of samples with larger variations in microbial loads, two linear calibration approaches, that is, MLR and PLSR, worked both in a satisfactory way (Tao et al., 2010). However, Tao et al. (2010) found that the presence of different micro flora would lead to changes in model precision, indicating the potential of HSI for identification of specific bacteria, where pathogens are to be predominantly considered. Apart from quantitative analyses, classification of meat freshness was conducted on chicken breasts (Grau et al., 2011). Besides, there is also work for freshness determination of fish, which showed the image acquisition modes employed, wavebands applied as well as the portion of the samples measured could lead to different model performance (Chau et al., 2009; Sivertsen et al., 2011).

In terms of detection of specific bacteria, Dubois et al. (2005) first isolated germs of interest from various food and developed food-specific cards, where a thick film of bacteria of each pure strain was filled in a well of the card. Instead of working on spectra, Dubois et al. (2005) analyzed the images at certain wavelengths in a way of simulating microbiological taxonomy. Therein, for each image, the distribution of pixel intensities was calculated and a threshold was carefully selected to separate one kind of bacteria from the others. Following such an approach with one strain isolated after statistics of each image at a specific wavelength, all bacteria were successfully identified in species level. The results obtained are encouraging, because they could offer a faster way for testing the presence of undesired target pathogens in certain food matrices compared to traditional standard methods. However, the speed can be further accelerated if complicated preparations can be reduced or omitted so that tests could be done directly on food. Siripatrawan et al. (2011) realized direct detection of bacteria on fresh spinach, and *E. coli* was precisely predicted with ANN and the prediction map showed clear distribution of the bacteria on the spinach leaves.

Fungal Contamination

Aflatoxin contaminated corns pose a serious threat to both humans and domestic animals because of mycotoxins, which are secondary metabolites that are toxic, immunosuppressant, and carcinogenic (Kalkan et al., 2011; Yao et al., 2005). Therefore, relevant laws or regulations have been established to mandate the control of fungal contamination, especially on cereal products. Meanwhile, the cereal industry is also looking for non-destructive, fast, and reliable methods for detecting fungal contamination. Hyperspectral imaging was initially investigated in visible-near infrared bands to identify healthy wheat kernels from those with scabs (Delwiche and Kim, 2000). In this study, band ratio involving two wavelengths within 425–860 nm was employed, and the result was encouraging. However, more bands were suggested to be included to attain better results. For the similar objective, efforts have also been devoted to classify wheat kernels into three categories, that is, normal, mildly infected, and severely damaged (Shahin and Symons, 2011).

In order to discriminate different fungi species on maize kernels, a tabletop-based spectral imaging system with waveband of 400–1000 nm was utilized by Del Fiore et al. (2010). In their study, during incubation of maize kernels that were inoculated with different fungi strains, the fungi-infected maize kernels could be identified as early as 48 h after inoculation. Instead of studying whole maize kernels, maize flour was investigated since the inspection of the delivery-ready products can help consolidate the last defending line for the sake of consumers. In this study, meanwhile, to enhance the detecting speed, a multispectral imaging system with 10 different LED lights spanning wavelengths ranging from 720 to 940 nm was explored by Firrao et al. (2010), who employed variance other than the average of reflectance values in specific area as input of calibration models. This algorithm required a reference image to assign pixels with similar light intensities into a corresponding group. Finally, the amount of fumonisin was successfully predicted using artificial neural network. Another quantitative analysis which correlated spectral profiles with concentration of *Fusarium* DNA was implemented on two hyperspectral imaging systems working under transmission mode in 430–900 nm and 900–1750 nm, respectively (Polder et al., 2005). Their results indicated that when predicting *Fusarium* DNA on wheat kernels, NIR spectral bands gave more useful information than the visible range, and it has the potential to produce satisfactory results with detection limit of 100 pg fungus DNA per wheat kernel. Later, more applications were found with HSI systems working with spectral range of 900–1700 nm. For example, Singh et al. (2007) employed a HSI system with an InGaAs camera and classified wheat kernels contaminated with storage fungi from healthy kernels. The results were that the healthy kernels could be separated from the infected kernels fairly well in a two-class classification, but when four-class classification was applied, no sound outcome was found for discriminating *Aspergillus glaucus*, and *Aspergillus niger*. On the same platform, this problem was improved by extracting various image parameters such as mean, variance, skewness, and kurtosis, and by adopting a pattern recognition method such as support vector machine, however, there was still 10% misclassification (Zhang et al., 2007). This system utilized by Singh et al. (2007) and Zhang et al. (2007) were simpler compared with other kits used because only 20 wavelengths were considered, which could be readily suitable for online inspection. Meanwhile, another report was available on recognizing wheat kernels using only one wavelength, with very good result (classification accuracy of 95%) being also obtained (Delwiche et al., 2009).

Fungal contamination has caused extensive attention from the cereal industry, but this also happens to other foodstuffs, such as hazelnuts, chili peppers, and apples. These products were also analyzed by HSI systems. For instance, Kalkan et al. (2011) classified hazelnuts and grounded red chili peppers into two classes, respectively, according to the corresponding allowed limits of aflatoxins present in food stipulated by EU Commission, which was different from normal classification of presence and absence.

Parasite Infections

In this part, parasites on or in fish will be discussed. Currently, parasites are removed from fish manually by inspection of fillets on candling tables (backlit tables). However, this method is not accurate, and only 60% to 70% of parasites can be recognized (Bublitz and Choudhury, 1992). A research group in Norway focused on quality and safety control of fish products, where detection of parasites is involved. Wold et al. (2001) first investigated a multispectral imaging system for its feasibility in detecting nematodes in cod fillets. They studied the spectral characteristics of different portions of the fillets (that is, blood spot, dark and white muscle, skin remnants, as well as

parasites), and carried out experiments to account for the effects of some factors including the color of parasites and their embedded depths, on the performance of classification models. In their study, parasites with different colors were successfully identified under a common model despite the obvious spectral discrepancy between parasites of distinctive colors (Stormo et al., 2007), but it was suggested to establish specific models that were competent for situations of different embedded depths. Additionally, different choices of calibration and post-processing methods can result in varying classification accuracy. For example, a larger threshold in discriminant partial least square (DPLS) tends to omit some targets of interest but bring in less false positives, while for a smaller threshold, a complete recognition of the targets may be at high cost of false positive, as illustrated by Heia et al. (2007). Similarly, cautions should also be taken to adjust the parameters for median filter, which is normally employed to reduce Type I errors. When Heia et al. (2007) applied median filtering with a filter size of 3×3 or 5×5, most of the impulse noise was removed after 1 run in both cases. Further, after a second run, the filters were capable of eradicating the impulse noise. However, at the same time, one of the parasites was also abandoned when the filer size was 5×5. Filter of 3×3 was then finally considered optimal since that specific worm was retained and no others were filtered. The studies mentioned above were all carried out in laboratory. Sivertsen et al. (2011); however, recently demonstrated the technical transfer from laboratory to industrial application. In lab scale, they followed the previously determined working condition (Heia et al., 2007) and adjusted the system with a new spectrometer in order to reduce the image acquisition time and enlarge the field of view. However, when the imaging areas were enlarged where the background was included, problems came consequently with the presence of severe artifacts in the images. As this problem was due to the projection of intense scattered light onto CCD sensors, which then led to blurred images, two alternatives were investigated aiming at reducing incoming direct light. It turned out to be more efficient to tilt the fiber light line than to assemble two linear polarizing filters because the latter reduced the intensities across the whole images, while the former only suppressed light saturation in the exterior of samples in the images, leaving the intensities in the middle portions of samples slightly reduced, which eventually improved the signal-to-noise ratio. Therefore, Sivertsen et al. (2011) tilted the fiber light line in their following pilot experiment. The overall result was satisfactory since this on-line system was capable of discriminating worms more efficiently than that by manual in industrial inspection line, though lots of false alarms were reported. This was a great step towards industrial application of HSI system for on-line detection of nematodes in fish fillets. However, more work is needed for better performance and faster speed. In addition, efforts should be devoted to improve data processing methods and experimental design (Sivertsen et al., 2011), or to extend the NIR band, which may offer more precise recognition as proved by Wold et al. (2001), who demonstrated that by eliminating large areas of false positives, the combination of NIR and visible bands produced a better discrimination of parasites than when NIR and visible bands were utilized separately.

Applications in Other Food Safety Problems

In protecting consumers from food-borne pathogens and hazards, it is also necessary to investigate other factors affecting the safety of food. Two examples studied using hyperspectral imaging are organic residues on food processing equipments and meat and bone meal (MBM) in feeds. Cho et al. (2007) applied a ratio algorithm in reflectance mode to detect the wet and dry organic residues, where both fecal contaminants and chicken residues such as fat and blood were included. In similar detection, Qin et al. (2011) used LED-induced hyperspectral fluorescence imaging. In monitoring MBM in feedstuffs for Bovine Spongiform Encephalopathy (BSE) diseases, several studies were implemented and most of them were conducted in near-infrared wavebands. Pierna et al. (2004) succeeded in discriminating MBM from vegetal particles using PLS, ANN, and SVM. In another work, Mahalanobis distance based discriminant analysis and PLSDA were also used (Riccioli et al., 2011; Wang and Paliwal, 2005). Abbas et al. (2010) also applied microscopic NIR imaging for MBM detecting. Furthermore, by exploring Vis-NIR band (419–892 nm), Nansen et al. (2010) developed a system that was able to classify MBM with contamination level as low as 1%.

CONCLUSIONS

This paper summarizes the application of hyperspectral imaging in food safety inspection and control. Hyperspectral imaging integrates two popular technologies, that is, spectroscopy and computer vision, to present both spectral and image information of food products at the same time. Such richness in information provides a broad platform for applying various chemometric algorithms and multivariate data analyses to reveal quality and safety parameters in the food commodities. Furthermore, this platform can be widened by introducing different spectral profiles, that is, NIR, Raman, and fluorescence spectra, and its effectiveness has been preliminarily confirmed in some aspects of food safety. However, as a promising technique, hyperspectral imaging should be expanded into more food safety fields to play a greater role in preventing outbreaks of food safety problems.

ACKNOWLEDGEMENTS

The authors would like to acknowledge China Scholarship Council (CSC) and University College Dublin (UCD) for financial support of this study under CSC-UCD Scheme. Dr. Amalia Scannell from UCD School of Agriculture & Food Science is gratefully thanked for kind suggestions.

REFERENCES

Abbas, O., Pierna, J. A. F., Dardenne, P., and Baeten, V. (2010). Near-infrared microscopic methods for the detection and quantification of processed by-products of animal origin. **In:** Sensing for Agriculture and Food Quality and Safety II. Proceedings of the SPIE, 7676: 767600-1-14. Kim, M. S., Tu, S.-I., and Chao, K.. (Eds.), Orlando, Florida, USA.

Ariana, D., Guyer, D. E., and Shrestha, B. (2006). Integrating multispectral reflectance and fluorescence imaging for defect detection on apples. *Computers and Electronics in Agriculture*. **50**: 148–161.

Ariana, D. P., Lu, R., and Guyer, D. E. (2006). Near-infrared hyperspectral reflectance imaging for detection of bruises on pickling cucumbers. *Computers and Electronics in Agriculture*. **53**: 60–70.

Bhuvaneswari, K., Fields, P. G., White, N. D. G., Sarkar, A. K., Singh, C. B., and Jayas, D. S. (2011). Image analysis for detecting insect fragments in semolina. *Journal of Stored Products Research*. **47**: 20–24.

Bolognesi, C. and Morasso, G. (2000). Genotoxicity of pesticides: potential risk for consumers. *Trends in Food Science & Technology*. **11**: 182–187.

Bonnier, F., Bertrand, D., Rubin, S., Venteo, L., Pluot, M., Baehrel, B., Manfait, M., and Sockalingum, G. D. (2008). Detection of pathological aortic tissues by infrared multispectral imaging and chemometrics. *Analyst*. **133**: 784–790.

Brosnan, T. and Sun, D. W. (2004). Improving quality inspection of food products by computer vision: A review. *Journal of Food Engineering*. **61**: 3–16.

Bublitz, C. G. and Choudhury, G. S. (1992). Effect of light intensity and color on worker productivity and parasite detection efficiency during candling of cod fillets. *Journal of Aquatic Food Product Technology*. **1**: 75–89.

Calnek, B. W., Barnes, H. J., W, B. C., Reid, W. M., and Yoder, H. W. (1991). Diseases of Poultry. Iowa State University Press, Ames, Iowa.

CDC (2011). Estimates of Foodborne Illness in the United States, http://www.cdc.gov/foodborneburden/2011-foodborne-estimates.html Accessed: September 29, 2011.

Cen, H. and He, Y. (2007). Theory and application of near infrared reflectance spectroscopy in determination of food quality. *Trends in Food Science & Technology*. **18**: 72–83.

Chao, K. (2010). Automated poultry carcass inspection by a hyperspectral-multispectral line-scan imaging system. **In:** Hyperspectral Imaging for Food Quality Analysis and Control, pp. 241–272. Sun, D.-W., Ed., Academic Press, San Diego.

Chao, K., Mehl, P., and Chen, Y. (2002). Use of hyper–and multi–spectral imaging for detection of chicken skin tumors. *Applied Engineering in Agriculture*. **18**: 113–119.

Chao, K., Qin, J., Kim, M. S., and Mo, C. Y. (2011). A Raman chemical imaging system for detection of contaminants in food **In:** Sensing for Agriculture and Food Quality and Safety III. Proceedings of SPIE, 8027: 802710-1-10. Kim, M. S., Tu, S.-I., and Chao, K., Eds., Orlando, FL.

Chao, K., Yang, C.-C., and Kim, M. S. (2010). Spectral line-scan imaging system for high-speed non-destructive wholesomeness inspection of broilers. *Trends in Food Science & Technology.* **21**: 129–137.

Chao, K., Yang, C., Chen, Y., Kim, M., and Chan, D. (2007a). Fast line-scan imaging system for broiler carcass inspection. *Sensing and Instrumentation for Food Quality and Safety*. **1**: 62–71.

Chao, K., Yang, C., Chen, Y., Kim, M., and Chan, D. (2007b). Hyperspectral-multispectral line-scan imaging system for automated poultry carcass inspection applications for food safety. *Poultry Science*. **86**: 2450.

Chao, K., Yang, C., Kim, M., and Chan, D. (2008). High throughput spectral imaging system for wholesomeness inspection of chicken. *Applied Engineering in Agriculture*. **24**: 475–485.

Chau, A., Whitworth, M., Leadley, C., and Millar, S. (2009). Innovative sensors to rapidly and non-destructively determine fish freshness Cambden BRI.

Cheng, X., Chen, Y., Tao, Y., Wang, C., Kim, M., and Lefcourt, A. (2004). A novel integrated PCA and FLD method on hyperspectral image feature extraction for cucumber chilling damage inspection. *Transactions of ASAE*. **47**: 1313–1320.

Chevallier, S., Bertrand, D., Kohler, A., and Courcoux, P. (2006). Application of PLS-DA in multivariate image analysis. *Journal of Chemometrics*. **20**: 221–229.

Chmiel, M., Słowiński, M., and Dasiewicz, K. (2011). Application of computer vision systems for estimation of fat content in poultry meat. *Food Control*. **22**: 1424–1427.

Cho, B.-K., Chen, Y.-R., and Kim, M. S. (2007). Multispectral detection of organic residues on poultry processing plant equipment based on hyperspectral reflectance imaging technique. *Computers and Electronics in Agriculture*. **57**: 177–189.

Cody, S. H., Glynn, M. K., Farrar, J. A., Cairns, K. L., Griffin, P. M., Kobayashi, J., Fyfe, M., Hoffman, R., King, A. S., and Lewis, J. H. (1999). An outbreak of Escherichia coli O157: H7 infection from unpasteurized commercial apple juice. *Annals of Internal Medicine*. **130**: 202–209.

Cubero, S., Aleixos, N., Moltó, E., Gómez-Sanchis, J., and Blasco, J. (2011). Advances in machine vision applications for automatic inspection and quality evaluation of fruits and vegetables. *Food and Bioprocess Technology*. **4**: 487–504.

Del Fiore, A., Reverberi, M., Ricelli, A., Pinzari, F., Serranti, S., Fabbri, A. A., Bonifazi, G., and Fanelli, C. (2010). Early detection of toxigenic fungi on maize by hyperspectral imaging analysis. *International Journal of Food Microbiology.* **144**: 64–71.

Delwiche, S. R., and Kim, M. S. (2000). Hyperspectral imaging for detection of scab in wheat. **In:** Biological Quality and Precision Agriculture II, Proceedings of SPIE. **4203**: 13–20. DeShazer, J. A. and Meyer, G. E. (Eds.), Boston, MA.

Delwiche, S. R., Yang, I. C., and Kim, M. S. (2009). Hyperspectral imaging for detection of black tip damage in wheat kernels. **In:** Sensing for Agriculture and Food Quality and Safety, Proceedings of SPIE, 7315: 73150K-1-6. Kim, M. S., Tu, S.-I., and Chao, K. (Eds.), Orlando, FL.

Desmond, E. M., Kenny, T. A., Ward, P., and Sun, D.-W. (2000). Effect of rapid and conventional cooling methods on the quality of cooked ham joints. *Meat Science.* **56**(3): 271–277

Du, C.-J. and Sun, D.-W. (2004). Recent developments in the applications of image processing techniques for food quality evaluation. *Trends in Food Science & Technology*. **15**: 230–249.

Du, Z., Jeong, M., and Kong, S. (2007). Band selection of hyperspectral images for automatic detection of poultry skin tumors. *IEEE Transactions on Automation Science and Engineering*. **4**: 332–339.

Dubois, J., Neil Lewis, E., Fry, J. F. S., and Calvey, E. M. (2005). Bacterial identification by near-infrared chemical imaging of food-specific cards. *Food Microbiology*. **22**: 577–583.

ElMasry, G., Barbin, D. F., Sun, D.-W., and Allen, P. (2011). Meat quality evaluation by Hyperspectral Imaging Technique: An overview. *Critical Reviews in Food Science and Nutrition.* (In Press)

ElMasry, G., Kamruzzaman, M., Sun, D.-W., and Allen, P. (2011). Principles and applications of hyperspectral imaging in quality evaluation of agro-food products: a review. *Critical Reviews in Food Science and Nutrition*. (In Press)

ElMasry, G. and Sun, D.-W. (2010). Principles of Hyperspectral Imaging Technology. **In:** Hyperspectral Imaging for Food Quality Analysis and Control, pp. 3–43. Sun, D.-W., Ed., Academic Press, San Diego.

ElMasry, G., Wang, N., Vigneault, C., Qiao, J., and ElSayed, A. (2008). Early detection of apple bruises on different background colors using hyperspectral imaging. *LWT-Food Science and Technology*. **41**: 337–345.

Firrao, G., Torelli, E., Gobbi, E., Raranciuc, S., Bianchi, G., and Locci, R. (2010). Prediction of milled maize fumonisin contamination by multispectral image analysis. *Journal of Cereal Science*. **52**: 327–330.

Fletcher, J. and Kong, S. (2003). Principal component analysis for poultry tumor inspection using hyperspectral fluorescence imaging. **In:** Proceedings of the International Joint Conference on Neural Networks, pp. 149–153.

Gómez-Sanchis, J., Martín-Guerrero, J. D., Soria-Olivas, E., Martínez-Sober, M., Magdalena-Benedito, R., and Blasco, J. (2012). Detecting rottenness caused by Penicillium genus fungi in citrus fruits using machine learning techniques. *Expert Systems with Applications*. **39**: 780–785.

Gowen, A., O'Donnell, C., Taghizadeh, M., Cullen, P., Frias, J., and Downey, G. (2008). Hyperspectral imaging combined with principal component analysis for bruise damage detection on white mushrooms (Agaricus bisporus). *Journal of Chemometrics*. **22**: 259–267.

Gowen, A. A., O'Donnell, C. P., Cullen, P. J., Downey, G., and Frias, J. M. (2007). Hyperspectral imaging - an emerging process analytical tool for food quality and safety control. *Trends in Food Science & Technology*. **18**:590–598.

Grau, R., Sánchez, A. J., Girón, J., Iborra, E., Fuentes, A., and Barat, J. M. (2011). Nondestructive assessment of freshness in packaged sliced chicken breasts using SW-NIR spectroscopy. *Food Research International*. **44**: 331–337.

Heia, K., Sivertsen, A. H., Stormo, S. K., Elvevoll, E., Wold, J. P., and Nilsen, H. (2007). Detection of nematodes in cod (Gadus morhua) fillets by imaging spectroscopy. *Journal of Food Science*. **72**: E11–E15.

Heitschmidt, G., Park, B., Lawrence, K., Windham, W., and Smith, D. (2007). Improved hyperspectral imaging system for fecal detection on poultry carcasses. *Transactions of the ASABE*. **50**: 1427–1432.

Heitschmidt, J., Lanoue, M., Mao, C., and May, G. (1998). Hyperspectral analysis of fecal contamination: A case study of poultry. **In:** Pathogen Detection and Remediation for Safe Eating, Proceedings of SPIE. **3544**: 134–137. Chen, Y. R. (Ed.), Boston. Massachusetts, 5 November, 1998.

Herrero, A. M. (2008). Raman spectroscopy a promising technique for quality assessment of meat and fish: A review. *Food Chemistry*. **107**: 1642–1651.

Jiang, L., Zhu, B., Rao, X., Berney, G., and Tao, Y. (2007). Discrimination of black walnut shell and pulp in hyperspectral fluorescence imagery using Gaussian kernel function approach. *Journal of Food Engineering*. **81**: 108–117.

Kalkan, H., Beriat, P., Yardimci, Y., and Pearson, T. C. (2011). Detection of contaminated hazelnuts and ground red chili pepper flakes by multispectral imaging. *Computers and Electronics in Agriculture*. **77**: 28–34.

Karoui, R. and Blecker, C. (2011). Fluorescence spectroscopy measurement for quality assessment of food systems: A review. *Food and Bioprocess Technology*. **4**: 364–386.

Kim, I., Kim, M., Chen, Y., and Kong, S. (2004a). Detection of skin tumors on chicken carcasses using hyperspectral fluorescence imaging. *Transactions of the ASAE*. **47**: 1785–1792.

Kim, I., Xu, C., and Kim, M. (2006). Poultry Skin Tumor Detection in Hyperspectral Images Using Radial Basis Probabilistic Neural Network. **In:** Advances in Neural Networks - ISNN 2006, pp. 770–776. Wang, J., Yi, Z., Zurada, J., Lu, B.-L., and Yin, H., Eds., Springer, Berlin.

Kim, M., Chao, K., Chen, Y., Chan, D., and MEHL, P. (2001a). Hyperspectral imaging system for food safety: Detection of fecal contamination on apples. **In:** Proceedings of SPIE. **4206**: 174–184. Chen, Y. R., and Tu, S.-I. (Eds.), Society of Photo-Optical Instrumentation Engineers, Boston, MA.

Kim, M., Chen, Y., Cho, B., Chao, K., Yang, C., Lefcourt, A., and Chan, D. (2007). Hyperspectral reflectance and fluorescence line-scan imaging for online defect and fecal contamination inspection of apples. *Sensing and Instrumentation for Food Quality and Safety*. **1**: 151–159.

Kim, M., Chen, Y., and Mehl, P. (2001b). Hyperspectral reflectance and fluorescence imaging system for food quality and safety. *Transactions of ASAE*. **44**: 721–729.

Kim, M., Lefcourt, A., Chao, K., Chen, Y., Kim, I., and Chan, D. (2002a). Multispectral detection of fecal contamination on apples based on hyperspectral imagery: Part I. Application of visible and near–infrared reflectance imaging. *Transactions of the ASAE*. **45**: 2027–2037.

Kim, M., Lefcourt, A., and Chen, Y. (2003). Multispectral laser-induced fluorescence imaging system for large biological samples. *Applied Optics*. **42**: 3927–3934.

Kim, M., Lefcourt, A., and Chen, Y. (2004b). Multispectral fluorescence imaging techniques for nondestructive food safety inspection. Monitoring Food Safety, Agriculture, and Plant Health, Proceedings of SPIE, **5271**: 62–72. Bennedsen, B. S., Chen, Y. -R., Meyer, G. E., Senecal, A. G., Tu, S.-I. (Eds.), Providence, RI.

Kim, M., Lefcourt, A., Chen, Y., Kim, I., Chan, D., and Chao, K. (2002b). Multispectral detection of fecal contamination on apples based on hyperspectral imagery: Part II. Application of hyperspectral fluorescence imaging. *Transactions of the ASABE*. **45**: 2039–2047.

Kise, M., Park, B., Lawrence, K., and Windham, W. (2008). Development of handheld two-band spectral imaging system for food safety inspection. *Biological Engineering*. **1**: 145–157.

Kong, S., Chen, Y., Kim, I., and Kim, M. (2004). Analysis of hyperspectral fluorescence images for poultry skin tumor inspection. *Applied Optics*. **43**: 824–833.

Kulmyrzaev, A., Bertrand, D., and Dufour, É. (2008). Characterization of different blue cheeses using a custom-design multispectral imager. *Dairy Science & Technology*. **88**: 537–548.

Lawrence, K., Park, B., Windham, W., and Mao, C. (2003). Calibration of a pushbroom hyperspectral imaging system for agricultural inspection. *Transactions of the ASABE*. **46**: 513–521.

Lawrence, K., Windham, W., Park, B., and Buhr, R. (2001). Hyperspectral imaging system for identification of fecal and ingesta contamination on poultry carcasses. 2001 ASAE Annual Meeting, Sacramento, CA.

Lawrence, K., Windham, W., and Smith, D. (2002). Contaminant detection on poultry carcass surfaces. *New Food*. **5**: 21–26.

Lawrence, K., Windham, W., Smith, D., Park, B., and Feldner, P. (2006). Effect of broiler carcass washing on fecal contaminant imaging. *Transactions of the ASABE*. **49**: 133–140.

Lawrence, K. C., Windham, W. R., Park, B., and Buhr, R. J. (2003). A hyperspectral imaging system for identification of fecal and ingesta contamination on poultry carcasses. *Journal of Near Infrared Spectroscopy*. **11**: 269–281.

Lee, K., Kang, S., Delwiche, S., Kim, M., and Noh, S. (2008). Correlation analysis of hyperspectral imagery for multispectral wavelength selection for detection of defects on apples. *Sensing and Instrumentation for Food Quality and Safety*. **2**: 90–96.

Lefcourt, A. M., Kim, M. S., and Chen, Y.-R. (2005a). Detection of fecal contamination on apples with nanosecond-scale time-resolved imaging of laser-induced fluorescence. *Appl. Opt.* **44**:1160–1170.

Lefcourt, A. M., Kim, M. S., and Chen, Y.-R. (2005b). A transportable fluorescence imagining system for detecting fecal contaminants. *Computers and Electronics in Agriculture*. **48**: 63–74.

Lefcourt, A. M., Kim, M. S., and Chen, Y. R. (2005c). Detection of fecal contamination in apple calyx by multispectral laser-induced fluorescence. *Transactions of ASAE*. **48**: 1587–1593.

Lefcout, A. M., and Kim, M. S. (2006). Technique for normalizing intensity histograms of images when the approximate size of the target is known: Detection of feces on apples using fluorescence imaging. *Computers and Electronics in Agriculture*. **50**: 135–147.

Lefcout, A. M., Kim, M. S., Chen, Y.-R., and Kang, S. (2006). Systematic approach for using hyperspectral imaging data to develop multispectral imagining systems: Detection of feces on apples. *Computers and Electronics in Agriculture*. **54**: 22–35.

Li, J., Xue, L., Liu, M., Wang, X., and Luo, C. (2010). Hyperspectral imaging technology for determination of dichlorvos residue on the surface of navel orange. *Chinese Optics Letters*. **8**: 1050–1052.

Liu, Y., Chao, K., Kim, M. S., Tuschel, D., Olkhovyk, O., and Priore, R. J. (2009). Potential of Raman Spectroscopy and imaging methods for rapid and routine screening of the presence of melamine in animal feed and foods. *Appl. Spectrosc.* **63**: 477–480.

Liu, Y., Chen, Y.-R., Kim, M. S., Chan, D. E., and Lefcourt, A. M. (2007). Development of simple algorithms for the detection of fecal contaminants on apples from visible/near infrared hyperspectral reflectance imaging. *Journal of Food Engineering*. **81**: 412–418.

Liu, Y., Chen, Y., Wang, C., Chan, D., and Kim, M. (2005). Development of a simple algorithm for the detection of chilling injury in cucumbers from visible/near-infrared hyperspectral imaging. *Applied Spectroscopy*. **59**: 78–85.

Liu, Y., Chen, Y., Wang, C., Chan, D., and Kim, M. (2006). Development of hyperspectral imaging technique for the detection of chilling injury in cucumbers: Spectral and image analysis. *Applied Engineering in Agriculture*. **22**: 101–111.

Liu, Y., Windham, W., Lawrence, K., and Park, B. (2003). Simple algorithms for the classification of visible/near-infrared and hyperspectral imaging spectra of chicken skins, feces, and fecal contaminated skins. *Applied Spectroscopy*. **57**: 1609–1612.

Lorente, D., Aleixos, N., Gómez-Sanchis, J., Cubero, S., and Blasco, J. (2011). Selection of optimal wavelength features for decay detection in citrus fruit using the ROC curve and neural networks. *Food and Bioprocess Technology*. DOI: 10.1007/s11947-011-0737-X.

Lu, R. (2003). Detection of bruises on apples using near-infrared hyperspectral imaging. *Transactions of the ASABE*. **46**: 523–530.

Lu, R., Chen, Y.-R., Park, B., and Choi, K.-H. (1999). Hyperspectral Imaging for Detecting Bruises in Apples **In:** ASAE Annual International Meeting, Paper No. 993120, St. Joseph, Michigan.

Lu, R. and Chen, Y. (1998). Hyperspectral imaging for safety inspection of food and agricultural products. **In:** Pathogen Detection and Remediation for Safe Eating, Proceedings of SPIE. **3544**: 121–133. Chen, Y.-R. (Ed), Boston, Massachusetts.

Lu, X., Al-Qadiri, H., Lin, M., and Rasco, B. (2011). Application of mid-infrared and Raman Spectroscopy to the study of bacteria. *Food and Bioprocess Technology*. **4**: 919–935.

Mauer, L. J., Chernyshova, A. A., Hiatt, A., Deering, A., and Davis, R. (2009). Melamine detection in infant formula powder using near- and mid-infrared spectroscopy. *Journal of Agricultural and Food Chemistry*. **57**: 3974–3980.

McDonald, K. and Sun, D.-W. (2001). Effect of evacuation rate on the vacuum cooling process of a cooked beef product. **48**(3): 195–202

McDonald, K., Sun, D.-W., and Kenny, T. (2001). The effect of injection level on the quality of a rapid vacuum cooled cooked beef product. **47**(2): 139–147

Mehl, P., Chao, K., Kim, M., and Chen, Y. (2001). Detection of contamination on selected apple cultivars using reflectance hyperspectral and multispectral analysis. **In:** Photonic Detection and Intervention Technologies for Safe Food Proceedings of SPIE. **4206**: 201–213. Chen, Y.-R., and Tu, S.-I. (Eds.), Boston, MA.

Mehl, P. M., Chen, Y.-R., Kim, M. S., and Chan, D. E. (2004). Development of hyperspectral imaging technique for the detection of apple surface defects and contaminations. *Journal of Food Engineering*. **61**: 67–81.

Menesatti, P., Zanella, A., D'Andrea, S., Costa, C., Paglia, G., and Pallottino, F. (2009). Supervised Multivariate Analysis of Hyper-spectral NIR Images to evaluate the starch index of apples. *Food and Bioprocess Technology*. **2**: 308–314.

Mohebbi, M., Akbarzadeh-T, M.-R., Shahidi, F., Moussavi, M., and Ghoddusi, H.-B. (2009). Computer vision systems (CVS) for moisture content estimation in dehydrated shrimp. *Computers and Electronics in Agriculture*. **69**: 128–134.

Nagata, M., Tallada, J. G., and Kobayashi, T. (2006). Bruise detection using NIR hyperspectral imaging for strawberry (Fragaria × ananassa Duch.*). Environment Control in Biology*. **44**: 133–142.

Nakariyakul, S. and Casasent, D. (2007). Fusion algorithm for poultry skin tumor detection using hyperspectral data. *Applied Optics*. **46**: 357–364.

Nakariyakul, S. and Casasent, D. P. (2009). Fast feature selection algorithm for poultry skin tumor detection in hyperspectral data. *Journal of Food Engineering*. **94**: 358–365.

Nansen, C., Herrman, T., and Swanson, R. (2010). Machine vision detection of bonemeal in animal feed samples. *Applied Spectroscopy*. **64**: 637–643.

Narendra, P. M. (1977). A branch and bound algorithm for feature subset selection. *IEEE Transactions on Computers*. **26**: 917–922.

Nicolaï, B. M., Lötze, E., Peirs, A., Scheerlinck, N., and Theron, K. I. (2006). Non-destructive measurement of bitter pit in apple fruit using NIR hyperspectral imaging. *Postharvest Biology and Technology*. **40**: 1–6.

Park, B., Kise, M., Lawrence, K., Windham, W., Smith, D., and Thai, C. (2007). Real-time multispectral imaging system for online poultry fecal inspection using unified modeling language. *Sensing and Instrumentation for Food Quality and Safety*. **1**: 45–54.

Park, B., Kise, M., Windham, W., Lawrence, K., and Yoon, S. (2008). Textural analysis of hyperspectral images for improving contaminant detection accuracy. *Sensing and Instrumentation for Food Quality and Safety*. **2**: 208–214.

Park, B., Lawrence, K., Windham, W., and Smith, D. (2004a). Multispectral imaging system for fecal and ingesta detection on poultry carcasses. *Journal of Food Process Engineering*. **27**: 311–327.

Park, B., Lawrence, K., Windham, W., and Smith, D. (2005). Detection of cecal contaminants in visceral cavity of broiler carcasses using hyperspectral imaging. *Applied Engineering in Agriculture*. **21**: 627–635.

Park, B., Lawrence, K., Windham, W., Smith, D., and Feldner, P. (2002). Hyperspectral imaging for food processing automation. **In:** Proceedings of SPIE, **4816**: 308–316. Sylvia S. Shen (Ed.), Seattle, WA.

Park, B., Lawrence, K. C., Windham, W. R., and Smith, D. P. (2006). Performance of hyperspectral imaging system for poultry surface fecal contaminant detection. *Journal of Food Engineering*. **75**: 340–348.

Park, B., Windham, W., Lawrence, K., and Smith, D. (2004b). Hyperspectral image classification for fecal and ingesta identification by spectral angle mapper. *ASAE Annual Meeting*, Ottawa, Canada.

Park, B., Windham, W. R., Lawrence, K. C., and Smith, D. P. (2007). Contaminant classification of poultry hyperspectral imagery using a spectral angle mapper algorithm. *Biosystems Engineering*. **96**: 323–333.

Park, B., Yoon, S.-C., R. , W. W., C., L. K., Heitschmidt, G. W., Kim, M. S., and Chao, K. (2011). Line-scan hyperspectral imaging for real-time poultry fecal detection. **In:** Proceedings of SPIE, pp. 76760I-76761-76710. Kim, M. S., Tu, S.-I., and Chao, K., Eds.

Park, B., Yoon, S.-C., Windham, W., and Lawrence, K. (2011). In-plant test of in-line multispectral imaging system for fecal detection during poultry processing. *Applied Engineering in Agriculture*. **27**: 623–630.

Park, B., Yoon, S.-C., Windham, W., Lawrence, K., Kim, M., and Chao, K. (2011). Line-scan hyperspectral imaging for real-time in-line poultry fecal detection. *Sensing and Instrumentation for Food Quality and Safety*. **5**: 25–32.

Peng, Y., Zhang, J., Wang, W., Li, Y., Wu, J., Huang, H., Gao, X., and Jiang, W. (2011). Potential prediction of the microbial spoilage of beef using spatially resolved hyperspectral scattering profiles. *Journal of Food Engineering*. **102**: 163–169.

Pierna, J. A. F., Baeten, V., Renier, A. M., Cogdill, R. P., and Dardenne, P. (2004). Combination of support vector machines (SVM) and near-infrared (NIR) imaging spectroscopy for the detection of meat and bone meal (MBM) in compound feeds. *Journal of Chemometrics*. **18**: 341–349.

Polder, G., Van der Heijden, G., Waalwijk, C., and Young, I. (2005). Detection of Fusarium in single wheat kernels using spectral imaging. *Seed Science and Technology*. **33**: 655–668.

Priore, R. J., Olkhovyk, O., Drauch, A., Treado, P., Kim, M., and Chao, K. (2009). Recent advances in chemical imaging technology for the detection of contaminants for food safety and security. **In:** Sensing for Agriculture and Food Quality and Safety. Proceedings of SPIE. **7315**: 731507-731501-731508. Kim, M. S., Tu, S.-I., and Chao, K. (Eds.), Orlando, FL.

Qin, J., Burks, T. F., Ritenour, M. A., and Bonn, W. G. (2009). Detection of citrus canker using hyperspectral reflectance imaging with spectral information divergence. *Journal of Food Engineering*. **93**: 183–191.

Qin, J., Chao, K., and Kim, M. S. (2010). Raman Chemical Imaging System for Food Safety and Quality Inspection. *Transactions of ASABE*. **53**: 1873–1882.

Qin, J., Chao, K., Kim, M. S., Kang, S., Cho, B.-K., and W. , J. (2011). Detection of organic residues on poultry processing equipment surfaces by led-induced fluorescence imaging. *Applied Engineering in Agriculture*. **27**: 153–161.

Qin, J. and Lu, R. (2008). Measurement of the optical properties of fruits and vegetables using spatially resolved hyperspectral diffuse reflectance imaging technique. *Postharvest Biology and Technology*. **49**: 355–365.

Riccioli, C., Pérez-Marín, D., Guerrero-Ginel, J. E., Saeys, W., and Garrido-Varo, A. (2011). Pixel selection for Near-Infrared Chemical Imaging (NIR-CI) discrimination between fish and terrestrial animal species in animal protein by-product meals. *Appl. Spectrosc.* **65**: 771–781.

Shahin, M. A. and Symons, S. J. (2011). Detection of Fusarium damaged kernels in Canada Western Red Spring wheat using visible/near-infrared hyperspectral imaging and principal component analysis. *Computers and Electronics in Agriculture*. **75**: 107–112.

Shao, Y., Bao, Y., and He, Y. (2011). Visible/near-infrared spectra for linear and nonlinear calibrations: A case to predict soluble solids contents and pH Value in peach. *Food and Bioprocess Technology*. **4**: 1376–1383.

Singh, C., Jayas, D., Paliwal, J., and White, N. (2007). Fungal detection in wheat using near-infrared hyperspectral imaging. *Transactions of the ASABE*. **50**: 2171–2176.

Siripatrawan, U., Makino, Y., Kawagoe, Y., and Oshita, S. (2011). Rapid detection of Escherichia coli contamination in packaged fresh spinach using hyperspectral imaging. *Talanta*. **85**: 276–281.

Sivertsen, A. H., Heia, K., Stormo, S. K., Elvevoll, E., and Nilsen, H. (2011). Automatic nematode detection in cod fillets (Gadus Morhua) by transillumination hyperspectral imaging. *Journal of Food Science*. **76**: S77–S83.

Sivertsen, A. H., Kimiya, T., and Heia, K. (2011). Automatic freshness assessment of cod (Gadus morhua) fillets by Vis/Nir spectroscopy. *Journal of Food Engineering*. **103**: 317–323.

Sowoidnich, K., Schmidt, H., Maiwald, M., Sumpf, B., and Kronfeldt, H.-D. (2010). Application of Diode-Laser Raman Spectroscopy for in situ investigation of meat spoilage. *Food and Bioprocess Technology*. **3**: 878–882.

Stormo, S. K., Sivertsen, A. H., Heia, K., Nilsen, H., and Elvevoll, E. (2007). Effects of single wavelength selection for anisakid roundworm larvae detection through multispectral imaging. *Journal of Food Protection*. **70**: 1890–1895.

Sugiyama, T., Sugiyama, J., Tsuta, M., Fujita, K., Shibata, M., Kokawa, M., Araki, T., Nabetani, H., and Sagara, Y. (2010). NIR spectral imaging with discriminant analysis for detecting foreign materials among blueberries. *Journal of Food Engineering*. **101**: 244–252.

Sun, D.-W. (2000). Inspecting pizza topping percentage and distribution by a computer vision method. *J Food Eng.* **44**(4): 245–249.

Sun, D.-W. (2008). Computer Vision Technology for Food Quality Evaluation. Academic Press / Elsevier, San Diego, California, USA.

Sun, D.-W. (2009). Infrared Spectroscopy for Food Quality Analysis and Control. Academic Press, Elsevier, San Diego, CA.

Sun, D.-W. (2010). Hyperspectral Imaging for Food Quality Analysis and Control. Academic Press,. Elsevier, San Diego, CA.

Tao, F.-F., Wang, W., Li, Y.-Y., Peng, Y.-K., Wu, J.-H., Shan, J.-J., and Zhang, L.-L. (2010). A rapid nondestructive measurement method for assessing the total plate count on chilled pork surface. *Spectroscopy and Spectral Analysis*. **30**: 3405–3409.

Tsuta, M., ElMasry, G., Sugiyama, T., Fujita, K., and Sugiyama, J. (2009). Comparison between linear discrimination analysis and support vector machine for detecting pesticide on spinach leaf by hyperspectral imaging with excitation-emission matrix. **In:** European Symposium on Artificial Neural Networks: Advances in Computational Intelligence and Learning, Bruges, Belgium.

Tsuta, M., Takao, T., Sugiyama, J., Yukihiro, W., and Sagara, Y. (2006). Foreign substance detection in blueberry fruits by spectral imaging. *Food Science and Technology Research*. **12**: 96–100.

Vargas, A., Kim, M., Tao, Y., Lefcourt, A., and Chen, Y. (2004). Safety inspection of cantaloupes and strawberries using multispectral fluorescence imaging techniques. 2004 ASAE Annual Meeting, Ottawa, Canada.

Vargas, A., Kim, M., Tao, Y., Lefcourt, A., Chen, Y., Luo, Y., Song, Y., and Buchanan, R. (2005). Detection of fecal contamination on cantaloupes using hyperspectral fluorescence imagery. *Journal of Food Science*. **70**: e471-e476.

Wang, H. H. and Sun, D. W. (2003). Assessment of cheese browning affected by baking conditions using computer vision. *Journal of Food Engineering*. **56**: 339–345.

Wang, W. and Paliwal, J. (2005). Potential of near-infrared hyperspectral reflectance imaging for screening of farm feed contamination. **In:** Photonic Applications in Biosensing and Imaging. **5969**: 644–653. Chan, T., Yu, W. C. W., Krull, K., Hornsey, U. J., Wilson, R. I., and Weersink, R. A. Eds., Proceeding of SPIE, Toronto, Canada.

Wang, W., Peng, Y.-K., and Zhang, X.-L. (2010). Study on modeling method of total viable count of fresh pork meat based on hyperspectral imaging system. *Spectroscopy and Spectral Analysis*. **30**: 411–415.

Wang, W., Peng, Y., Huang, H., and Wu, J. (2011). Application of hyper-spectral imaging technique for the detection of total viable bacteria count in pork. *Sensor Letters*. **9**: 1024–1030.

Wang, W., Thai, C., Li, C., Gitaitis, R., Tollner, E., and Yoon, S. (2009). Detection of sour skin diseases in vidalia sweet onions using near-infrared hyperspectral imaging. *2009 ASAE Annual Meeting*, Reno, NV.

Wilcock, A., Pun, M., Khanona, J., and Aung, M. (2004). Consumer attitudes, knowledge and behaviour: A review of food safety issues. *Trends in Food Science & Technology*. **15**: 56–66.

Windham, W., Heitschmidt, G., Smith, D., and Berrang, M. (2005). Detection of ingesta on pre-chilled broiler carcasses by hyperspectral imaging. *International Journal of Poultry Science*. **4**: 959–964.

Windham, W., Lawrence, K., Park, B., Smith, D., and Poole, G. (2002). Analysis of reflectance spectra from hyperspectral images of poultry carcasses for fecal and ingesta detection. **In:** Proceedings of SPIE. **4816**: 317–324. Sylvia S. Shen (Ed.), Seattle, WA.

Windham, W., Smith, D., Berrang, M., Lawrence, K., and Feldner, P. (2005). Effectiveness of hyperspectral imaging system for detecting cecal contaminated broiler carcasses. *International Journal of Poultry Science*. **4**: 657–662.

Wold, J. P., Westad, F., and Heia, K. (2001). Detection of parasites in cod fillets by using SIMCA classification in multispectral images in the visible and NIR region. *Applied Spectroscopy*. **55**: 1025–1034.

Wu, D., He, Y., Feng, S. J., and Sun, D.-W (2008). Study on infrared spectroscopy technique for fast measurement of protein content in milk powder based on LS-SVM. *J Food Eng.* **84**(1): 124–131.

Wu, Y.-N., Zhao, Y.-F., and Li, J.-G. (2009). A survey on occurrence of melamine and its analogues in tainted infant formula in China. *Biomedical and Environmental Sciences*. **22**: 95–99.

Xing, J., Bravo, C., Jancsók, P. T., Ramon, H., and De Baerdemaeker, J. (2005). Detecting bruises on "Golden Delicious" apples using hyperspectral imaging with multiple wavebands. *Biosystems Engineering*. **90**: 27–36.

Xing, J. and De Baerdemaeker, J. (2005). Bruise detection on 'Jonagold' apples using hyperspectral imaging. *Postharvest Biology and Technology*. **37**: 152–162.

Xing, J., Saeys, W., and De Baerdemaeker, J. (2007). Combination of chemometric tools and image processing for bruise detection on apples. *Computers and Electronics in Agriculture*. **56**: 1–13.

Xu, C., Kim, I., and Kim, M. (2007). Poultry skin tumor detection in hyperspectral reflectance images by combining classifiers. **In:** Image Analysis and Recognition, pp. 1289–1296. Kamel, M., and Campilho, A., Eds., Springer, Berlin.

Xue, L., Li, J., and Liu, M. (2008). Detecting pesticide residue on navel orange surface by using hyperspectral imaging. *Acta Optica Sinica*. **28**: 2277–2280.

Yang, C.-C., Chao, K., Chen, Y.-R., and Early, H. L. (2005). Systemically diseased chicken identification using multispectral images and region of interest analysis. *Computers and Electronics in Agriculture*. **49**: 255–271.

Yang, C.-C., Kim, M., Kang, S., Tao, T., Chao, K., Lefcourt, A., and Chan, D. (2011). The development of a simple multispectral algorithm for detection of fecal contamination on apples using a hyperspectral line-scan imaging system. *Sensing and Instrumentation for Food Quality and Safety*. **5**: 10–18.

Yang, C.-C., Kim, M. S., Kang, S., Cho, B.-K., Chao, K., Lefcourt, A. M., and Chan, D. E. (2012). Red to far-red multispectral fluorescence image fusion for detection of fecal contamination on apples. *Journal of Food Engineering*. **108**: 312–319.

Yang, C., Chao, K., and Chen, Y. (2005). Development of multispectral image processing algorithms for identification of wholesome, septicemic, and inflammatory process chickens. *Journal of Food Engineering*. **69**: 225–234.

Yang, C., Jun, W., Kim, M., Chao, K., Kang, S., Chan, D., and Lefcourt, A. (2010a). Classification of fecal contamination on leafy greens by hyperspectral imaging. **In:** Sensing for Agriculture and Food Quality and Safety II, Proceedings of the SPIE. **7676**: 76760F-1-8. Orlando, FL.

Yang, C. C., Chao, K., Chen, Y. R., Kim, M. S., and Chan, D. E. (2006). Development of fuzzy logic based differentiation algorithm and fast line-scan imaging system for chicken inspection. *Biosystems Engineering*. **95**: 483–496.

Yang, C. C., Chao, K., Chen, Y. R., Kim, M. S., and Early, H. L. (2006). Simple multispectral image analysis for systemically diseased chicken identification. *Transactions of ASABE*. **49**: 245–257.

Yang, C. C., Jun, W., Kim, M. S., Chao, K., Kang, S., Chan, D. E., and Lefcourt, A. (2010b). Classification of fecal contamination on leafy greens by hyperspectral imaging. **In:** Sensing for Agriculture and Food Quality and Safety II, Proceedings of the SPIE, p. 76760F. Kim, M. S., Tu, S.-I., and Chao, K., Eds.

Yao, H., Hruska, Z., DiCrispino, K., Brabham, K., Lewis, D., Beach, J., Brown, R., and Cleveland, T. (2005). Differentiation of fungi using hyperspectral imagery for food inspection. *2005 ASAE Annual Meeting*. Tampa, FL.

Yao, H. and Lewis, D. (2010). Spectral Preprocessing and Calibration Techniques. **In:** Hyperspectral Imaging for Food Quality Analysis and Control, pp. 45–78. Sun, D.-W., Ed., Academic Press, San Diego.

Yoon, S., Lawrence, K., Park, B., and Windham, W. (2007). Statistical model-based thresholding of multispectral images for contaminant detection on poultry carcasses. *Transactions of the ASABE*. **50**: 1433–1442.

Yoon, S., Lawrence, K., Smith, D., Park, B., and Windham, W. (2006). Bone fragment detection in chicken breast fillets using back-illuminated structured light. *2006 ASAE Annual Meeting*. Portland, OR.

Yoon, S., Lawrence, K., Smith, D., Park, B., and Windham, W. (2008a). Bone fragment detection in chicken breast fillets using transmittance image enhancement. *Transactions of the ASABE*. **51**: 331–339.

Yoon, S., Lawrence, K., Smith, D., Park, B., and Windham, W. (2008b). Embedded bone fragment detection in chicken fillets using transmittance image enhancement and hyperspectral reflectance imaging. *Sensing and Instrumentation for Food Quality and Safety*. **2**: 197–207.

Zhang, H., Paliwal, J., Jayas, D., and White, N. (2007). Classification of fungal infected wheat kernels using near-infrared reflectance hyperspectral imaging and support vector machine. *Transactions of the ASABE*. **50**: 1779–1785.

Zheng, C., Sun, D.-W., and Zheng, L. (2006a). Recent applications of image texture for evaluation of food qualities: A review. *Trends in Food Science & Technology*. **17**: 113–128.

Zheng, C., Sun, D.-W., and Zheng, L. (2006b). Recent developments and applications of image features for food quality evaluation and inspection: A review. *Trends in Food Science & Technology*. **17**: 642–655.